Since January 2020 Elsevier has created a COVID-19 resource centre with free information in English and Mandarin on the novel coronavirus COVID-19. The COVID-19 resource centre is hosted on Elsevier Connect, the company's public news and information website.

Chemico-Biological Interactions 352 (2022) 109776

Contents lists available at ScienceDirect

Chemico-Biological Interactions

journal homepage: www.elsevier.com/locate/chembioint

Understanding immune-modulatory efficacy *in vitro*

Somanjana Khatua [a,b], Jesus Simal-Gandara [c,*], Krishnendu Acharya [a,**]

[a] *Molecular and Applied Mycology and Plant Pathology Laboratory, Centre of Advanced Study, Department of Botany, University of Calcutta, 35, Ballygunge Circular Road, Kolkata, 700019, West Bengal, India*

[b] *Department of Botany, Krishnagar Government College, Krishnagar, Nadia, 741101, West Bengal, India*

[c] *Universidade de Vigo, Nutrition and Bromatology Group, Department of Analytical Chemistry and Food Science, Faculty of Science, E-32004, Ourense, Spain*

ARTICLE INFO

Keywords:
Anti-inflammation
Immune enhancing
Macrophage cell lines
Modern techniques
Primer sequences
Principle of methods

ABSTRACT

Boosting or suppressing our immune system represents an attractive adjunct in the treatment of infections including SARS-CoV-2, cancer, AIDS, malnutrition, age related problems and some inflammatory disorders. Thus, there has been a growing interest in exploring and developing novel drugs, natural or synthetic, that can manipulate our defence mechanism. Many of such studies, reported till date, have been designed to explore effect of the therapeutic on function of macrophages, being a key component in innate immune system. Indeed, RAW264.7, J774A.1, THP-1 and U937 cell lines act as ideal model systems for preliminary investigation and selection of dose for *in vivo* studies. Several bioassays have been standardized so far where many techniques require high throughput instruments, cost effective reagents and technical assistance that may hinder many scholars to perform a method demanding compilation of available protocols. In this review, we have taken an attempt for the first time to congregate commonly used *in vitro* immune-modulating techniques explaining their principles. The study detected that among about 40 different assays and more than 150 sets of primers, the methods of cell proliferation by MTT, phagocytosis by neutral red, NO detection by Griess reaction and estimation of expression of TLRs, COX-2, iNOS, TNF-α, IL-6 and IL-1β by PCR have been the most widely used to screen the therapeutics under investigation.

1. Introduction

In human, the immune system is equipped to fight off invading wide array of potential pathogens that may cause diseases. For the last 70 years, the health sector has heavily relied on antimicrobial drugs that has now resulted in generation of multiple-drug-resistant bacteria [1]. In that note, therapeutic strategies based on improving the defence mechanism have several advantages over the use of traditional antibiotics [2]. In fact, administration of immune boosters may circumvent the problem of rapid emergence of resistant variety. The therapeutics may also expand treatment options for immunocompromised patients such as people suffering from certain types of cancer, AIDS, malnutrition, chronic granulomatous disease or age-related problems as well as in the advent of a novel pathogen [3]. As of March 2020, the world is currently dealing with a global outbreak of Coronavirus disease 2019 (COVID-19) caused by SARS-CoV-2, a new and different virus, and thus the existing vaccines are ineffective against it [4]. Scientists have suggested few approaches to counteract the infection where boosting the immune response in phase 1 has been found to be appropriate in addition to symptomatic treatment [5]. However, massive production of inflammatory cytokines by aberrant immune activation may in turn cause damage to host tissues. The situation emerges in the late stage of coronavirus disease where cytokine storm is a major reason for disease progression and eventual death [6]. Thus, administration of powerful anti-inflammatories that can suppress immune system along with antiviral drug could be effective in phase 2 [5]. The efficacy of nonsteroidal anti-inflammatory medications has also been documented in a number of clinical disorders, including rheumatoid arthritis, psoriasis, Crohn's disease, ulcerative colitis, gout, ankylosing spondylitis, dental pain, dysmenorrhea and headache [7].

On the whole, immunotherapy or biological therapy is the treatment of diseases, designed either to amplify an immune response, called immune-stimulation or reduce the response, called suppression immunotherapies [8]. Currently, there is a greater interest in natural compounds, such as dietary supplement and herbal remedies, which have been used for centuries as immune-modulators. Marine sources with

* Corresponding author.
** Corresponding author.
E-mail addresses: jsimal@uvigo.es (J. Simal-Gandara), krish_paper@yahoo.com (K. Acharya).

https://doi.org/10.1016/j.cbi.2021.109776
Received 24 July 2021; Received in revised form 19 November 2021; Accepted 7 December 2021
Available online 11 December 2021

diverse constituents (sulphated polysaccharide, terpenes, cyclic depsipeptide, polysaccharides, bioglycan, polyhydroxylated lactone, macrocyclic lactones, cyclic tripeptide) and medicinal plants with various active components (flavonoids, curcumin, saponin, carotenoids, alkaloid, tannic acid, tocopherol, polyphenol, ascorbate, polysaccharides) have proved their innate immune boosting abilities [8,9]. Fungi have also emerged as potential source of body defence enhancers where polysaccharides (in particular β-D-glucans), polysaccharopeptides and proteins have been recognized as bioactive compounds. Indeed, several mushroom derived macromolecules namely Schizophyllan, Lentinan, Krestin and polysaccharide-protein complex are now available as biological response modifiers in market [10]. On the other hand, alkaloids, glycosides, terpenoids, polyphenols, resins, essential oil, flavonoids, phenolic compounds, cannabinoids, steroids, fatty acids, lignans and glycoproteins isolated from various bio-resources have shown significant anti-inflammatory activities [11]. Numerous metal and metal oxide nanoparticles such as gold, silver, titanium dioxide, zinc oxide and selenium have also demonstrated to possess the medicinal prospect [12]. Most of these ingredients have been evaluated using *in vitro* system where macrophage cell lines are popularly used as an experimental model [13]. The monocytes can effortlessly be maintained; as a result, they are gradually being recognized as an ideal system for studies of immunomodulation and immunomechanics [14].

To date, a variety of *in vitro* immune modulating assays have been standardized to determine effect of a drug on specific function of macrophages, as published in our previous articles [15–20]. One-dimension approach can provide unequivocal result; thus, performing various methods is the best solution to reach the conclusion. However, most of these techniques are associated with instrumental, technical and practical limitations hindering researchers to perform an assay. It is thus important to have a complete knowledge about alternative methods targeting the same output. Therefore, a compiled description of all available *in vitro* models is an extreme requirement. In this regard, we intended to congregate the most commonly performed assays, suitable to estimate either immune-stimulatory or anti-inflammatory potency, as they execute opposite responses of the same method (Supplementary Fig. 1). The present review is expected to be highly beneficial not only to all immunologists to design new methods but also to pharmacists and biologists to develop novel drugs by selecting convenient assays.

2. Detection of lipopolysaccharide (LPS) contamination

The major contaminant found in biological substances is endotoxin, also called LPS, derived from cell membrane of Gram negative bacteria. Lipopolysaccharide is known to activate the immune system specifically macrophages with release of different pro-inflammatory mediators; as a result, LPS (generally at 5 μg/ml concentration) is used as a positive control in all immune-stimulation assays [17,21]. Thus, it is essential to detect presence of endotoxin in pharmaceutical products to understand sole effect of the drug. The commonly followed technique in this context is Limulus Amoebocyte Lysate (LAL) assay based on clotting ability of *Limulus polyphemus* blood upon exposure to endotoxin [22]. Briefly, 100 μl of test sample (10 mg/ml) or standard (positive control) or endotoxin-free water (negative control) are mixed with 100 μl of LAL for 1 h at 37 °C [23]. Gel is formed in proportional to endotoxin sensitivity

Table 1
Overview of some commonly used cell lines in immunomodulatory research [13,29–31]. The publication numbers were derived by searching in PubMed (https://www.ncbi.nlm.nih.gov/pubmed/) on November 18, 2021 using the following criteria: (i) RAW 264.7 AND immune activation; (ii) RAW 264.7 AND anti inflammation; (iii) J774 AND immune activation; (iv) J774 AND anti inflammation; (v) THP-1 AND immune activation; (vi) THP-1 AND anti inflammation; (vii) U937 AND immune activation; (viii) U937 AND anti inflammation; (vi) THP-1 AND anti inflammation; (ix) HL-60 AND immune activation; (x) HL-60 AND anti inflammation.

Cell lines	RAW264.7	J774.A1	THP-1	U937	HL-60
Source	BALB/c Mouse	BALB/c Mouse	Human	Human	Human
Establishing year	1978	1968	1980	1976	1977
Gender of the source	Male	Female	Male	Male	Female
Disease	Abelson murine leukemia virus-induced tumor	Reticulum sarcoma	Acute monocytic leukemia	Histiocytic lymphoma	Acute myeloid leukemia
Doubling time	~11 h	~17 h	~26 h	48–72 h	20–45 h
Growth mode	Semi-adherent	Semi-adherent	Suspension	Suspension	Suspension
Morphology	Loosely adherent, slightly spindle-shaped cells. Cells pile and become round shaped, when the culture is dense.	Round shaped cell with a large nucleus	Large, round single-cell morphology	Round shaped with short microvilli and a large beam-shaped nucleus	Round or ovoid, heterogeneous in size, occasionally express pseudopods
Other characters	High expression of iNOS in comparison with J774.A1	Gene expression profile is closer to mice peritoneal macrophages than RAW 264.7.	High phagocytic ability and expression of cell surface markers such as TLR-2, CD36, CD-14, and CR3 163 (CD11b/CD18)	Bears t (10; 11) (p13; q14) translocation, constitutively express high level of cell-surface HLA class I molecules	Contains an amplified *c-myc* proto-oncogene; *c-myc* mRNA level is high in undifferentiated cells and declines after differentiation. Expression of surface markers changes based on differentiation.
Commonly used assays	Cell viability, phagocytosis, measurement of NO, ROS and cytokines production, morphological analysis, estimation of gene and protein expression	Cell viability, phagocytosis, measurement of NO and cytokines production, morphological analysis, immunoblotting	Cell viability, phagocytosis, measurement of NO, ROS and cytokines production, estimation of gene and protein expression	Cell viability, phagocytosis, measurement of NO and cytokines production, estimation of gene and protein expression	Cell viability, measurement of NO, ROS and cytokines production, western blotting
No. of publications in immune-stimulatory field	2674	450	2519	1338	881
No. of publications in anti-inflammatory field	3843	175	1403	446	226

HLA: Human leucocyte antigen; NO: Nitric oxide; PMA: Phorbol-12-myristate-13-acetate; ROS: Reactive oxygen species; TLR: Toll-like receptor.

and 0.5 endotoxin unit (EU)/ml concentration is considered as the threshold level [22].

3. Cell culture

Murine macrophage cell lines such as RAW264.7 and J774A.1 are well-established typical systems in immunology and cell biology for their multi-tasking aptitude (Table 1). J774A.1 cell line was established from a female BALB/c/NIH mouse with a reticulum cell sarcoma [24]. These cells are cultured in Dulbecco's Modified Eagle's Medium (DMEM) or Roswell Park Memorial Institute (RPMI)-1640 medium supplemented with 10% fovin serum albumin (FBS), 100 μg/ml streptomycin and 100 units/ml penicillin at 37 °C in 5% CO_2 humidified atmosphere cultivator. The same condition can be used for culturing RAW264.7 macrophage cells. The cell line was constituted by SW Russell from ascites of a male BALB/c mouse bearing a tumor induced by Abelson murine leukemia virus [13]. Generally, the cells are cultivated for 36–48 h to reach the logarithmic phase and then used for experiments. Another option could be THP-1 (human acute monocytic leukemia derived cell line) or U937 (human myelomonocytic tumor), which differentiate into macrophages after exposure to phorbol-12-myristate-13-acetate (PMA) or a combination of PMA and LPS [25]. Next to these cells is HL-60 (human myelogenous leukemic cell line) that can be induced to differentiate *in vitro* into monocyte/macrophage-like cells, granulocyte-like cells and eosinophils after treatment with definite chemicals. As such, the cells are known to be differentiated into maturing macrophages in exposure with various differentiation-inducing agents such as 1,25-dihydroxyvitamin D_3, phorbol esters and sodium butyrate. While, dimethyl sulfoxide (DMSO) or all trans retinoic acid treatment induces HL-60 cells to differentiate to neutrophil-like cell [26]. Another less commonly used cell line is PLB-985, established in 1985, which was later identified as a sub-line of HL-60 and thus exhibit similar properties [27]. Comparatively, most of the experimentations have been performed using murine monocytes which might be due to fast growth rate and less variability of macrophages from *Mus musculusis* than that of *Homo sapiens* [28].

4. Determination of cell density by trypan blue dye exclusion test

Confluency of cells in culture causes slowdown of metabolism, decrease in cell division and contact inhibition of growth. As a result, the condition may lead to loss of linearity between cell number and effect of drug. So, starting an investigation with definite number of viable cells is vital to perform successful experiments. In this context, trypan blue dye exclusion test is the most commonly utilized assay to distinguish live and dead cells selectively [32]. This negatively charged diazo stain interacts with cells only when the membrane is disrupted. Indeed, the dye is capable to penetrate the cytoplasm of dead cells only. As a result, these cells appear with distinctive blue colour when observed under a microscope. In contrast, live cells with intact membrane exclude such stain allowing discrimination with non-viable cells [33]. However, the process cannot be used to differentiate healthy cells and cells that are alive but losing functions. To perform the assay, 0.4% (w/v) trypan blue solution is prepared in phosphate buffered solution or PBS (pH 7.2). In a microtube, 20 μl of the solution is mixed with 20 μl of cell suspension and 10 μl is loaded onto a haemocytometer. Viable and non-viable cells, represented as transparent and blue colour respectively, are counted following standard manner within 5 min of mixing [34]. For healthy log-phase culture, cell viability should be at least 95% and these cells can be used for further experimentation.

5. Cytotoxicity/cell proliferation assay

Cell viability and cytotoxicity studies are valuable tools for sensitivity testing of chemicals that also provide preliminary information for *in vivo* studies. A variety of methods have been developed so far to determine proliferation in mammalian cells. These techniques are established on measurement of cellular DNA content, direct counting of viable cells by trypan blue dye or estimation of metabolic activity [35]. The latter procedure is based on mitochondrial dehydrogenase activity and hence is reliable, accurate, easy-to-use, safe and far superior to other assays. In this note, a range of stains have been developed that produce a specific colour (Fig. 1). Generally, the monocytes are cultured at a density of 1×10^4 cells/well in 96-well plate overnight and then treated with stimulus. Following incubation, substrate is added and the ultimate colour intensity is measured by enzyme-linked immune sorbent assay (ELISA) plate reader. The cell viability can be calculated by using following equation:

$$\text{Index of proliferation} = (A - B)/(C - B)$$

Where A is optical density (OD) of the treated cells; B is OD of control wells (culture medium without cells); and C is OD of negative control (culture medium with cells). Non-cytotoxic concentrations of sample are selected to conduct downstream immune-stimulating assessments.

5.1. MTT

The MTT (3-(4,5-dimethyl-2-thiazolyl)-2,5-diphenyl-2H-tetrazolium bromide) assay was first described in 1983 and gradually has been modified by different authors. The method is based on reduction of yellow coloured water soluble MTT by mitochondrial succinate dehydrogenase activity in living cells into insoluble dark blue or purple formazan product [35–38]. The technique thus has great applicability for detection of metabolically active cells; even if they are not dividing. However, the disadvantage of the method is that the final product, formazan crystals injure cells and requires an organic solvent (DMSO or HCl/isopropanol) for solubilisation [38]. To perform the assay, 20 μl from MTT solution (5 mg/ml prepared in media or PBS) is added to each well to make final concentration of 0.5 mg/ml. After 4 h incubation at 37 °C, the supernatant is discarded and 150 μl DMSO is added. The plate is incubated for 10 min with frequent shaking to ensure complete solubilisation and absorbance is measured at 570 nm [39]. Else, 50 μl MTT stop solution (10% SDS in 10 mM HCl) can be added instead of DMSO followed by incubation for 24 h and measurement of absorbance at 540 nm [40].

5.2. MTS

MTS (3-(4,5-dimethylthiazol-2-yl)-5-(3-carboxymethoxyphenyl)-2-(4-sulfophenyl)-2H-tetrazolium), also called as Owen's reagent, is a weakly acidic inner salt closely related to MTT. This less toxic component is a negatively charged compound that cannot readily penetrate cells. So, the reagent is applied in combination with electron acceptor either phenazine methyl sulfate (PMS) or phenazine ethyl sulfate (PES). These intermediates can enter cell surface and exit cells to convert MTS to formazan product which is highly soluble in culture media. This transformation is thought to be accomplished by NADP(H)-dependent dehydrogenase enzyme in metabolically active cells [38]. Generally, 20 μl of MTS containing PES reagent is added in each well at the final concentration of 0.33 mg/ml. After 2 h incubation, the absorbance is determined at 490–500 nm using microplate reader [41].

5.3. WST

Recently, a new generation of water soluble tetrazolium salts has been developed of which WST-1 (4-[3-(4-iodophenyl)-2-(4-nitrophenyl)-2H-5-tetrazolio]-1,3-benzene disulfonate) is the prototype [42]. WST-1 is a negatively charged disulfonated inner salt containing an iodine residue that yields a highly water soluble formazan extracellularly in presence of NADH and an electron mediator such as 1-methoxy

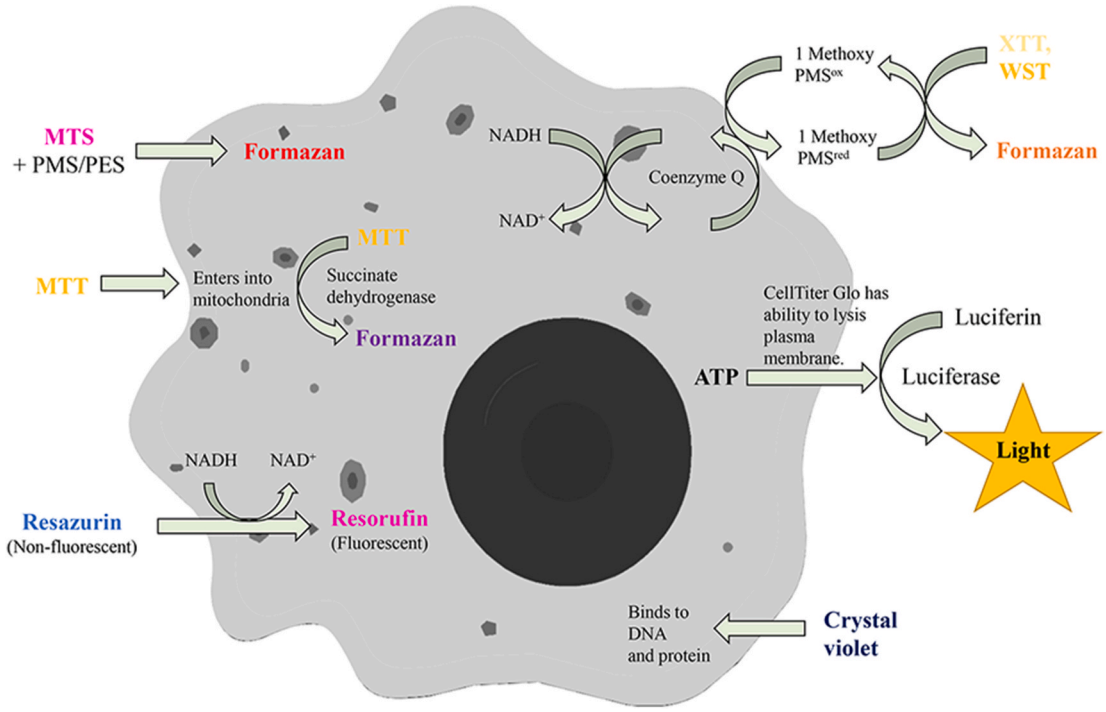

Fig. 1. Schematic representation of assays available for the detection of cell viability/proliferation of macrophage.

PMS [43]. With the advantage over conventional tetrazolium salts that both WST-1 and its formazan are very stable in solution and they have extremely low cytotoxicity. Till date, several other tetrazolium salts have been developed in WST series, perhaps the most useful being WST-8 and is being marketed independently as Cell Counting Kit-8 (CCK-8). Since, WST-8, formazan product and mPMS have no cytotoxicity in cell culture media, additional experiments may be carried out using the same cells from the previous assay [38]. In general, 20 μl of WST-1 or 10 μl in case of CCK-8 solution is added to 200 μl reaction mixture in each well and optical density is measured at 450 nm after 4 h incubation at 37 °C [44].

5.4. XTT

XTT (sodium 3-[1-(phenylaminocarbonyl)-3,4-tetrazolium]-bis(4-methoxy-6-nitro) benzene sulfonic acid hydrate) cell proliferation assay was first described in 1988 as an effective method to measure cell growth and drug sensitivity in tumour cell lines. The compound contains two sulfonate groups giving them a net negative charge that allows excluding them from cells. Thus, XTT dye reduction occurs at the cell surface facilitated by *trans*-plasma membrane electron transport and the colourless or slightly yellow compound is converted to brightly orange, soluble formazan product. This colour change is accomplished by breaking apart the positively charged quaternary tetarzole ring [45]. To perform the assay, 50 μl of XTT solution is added to each well for 10 h at 37 °C in 5% CO_2 incubator and the optical density is measured at 490 nm [46].

5.5. Alamar blue

Resazurin (7-hydroxy-10-oxido-phenoxazin-10-ium-3-one) is a redox dye that has been applied to assess microbial contamination in milk and biological fluids since 1950s [45]. The assay is based on entry of resazurin (non-fluorescent blue coloured) into cytosol where it accepts electron from NADH, NADPH, FMNH, FADH and cytochromes. As a result, the dye is reduced to red coloured, highly fluorescent compound namely resorufin. The result can be depicted using a fluorescence detector with 545/15 nm excitation and 580/10 nm emission wavelength [37]. Major advantage of the method is non-toxicity to cells and high stability in culture media allowing continue monitoring of cultures over time. Consequently, the dye became commercially available since 1993 in the name of AlamarBlue or vibrant or UptiBlue. At first, Resazurin solution is prepared by dissolving the reagent in PBS (0.001% w/v) or in DMEM (10%) in dark and sterile filtered (0.22 μm). Then, the treated media is aspirated, replaced with 100 μl of resazurin solution in each well and resultant fluorescence is measured after 1–2 h incubation [47,48].

5.6. CellTiter-Glo

CellTiter-Glo utilizes the ability of metabolically active cells to catalyse luciferase reaction by its own ATP, yielding a measurable product. The reagent has ability to lysis cell membranes to release ATP and inhibit endogenous ATPases so that no further ATP is synthesized. The chemical also provides luciferin and luciferase to initiate bioluminescent reaction with the help of ATP discharged from cells; whereby intensity of final product directly signifies the number of living cells [36]. To perform the assay, cells are allowed to equilibrate for 30 min at room temperature (RT) after treatment. Then, substrate is added and samples are analysed with a Fluoroscan [49].

5.7. Crystal violet

The technique was initially established for cell number measurement in monolayer cultures. It is a simple, non-enzymatic assay for quick analysis of quantity of viable adherent cells and colonies. The assay takes advantage of affinity between dye and external surface of DNA double helix [36]. While, disadvantage of the assay is that if all dead cells are not removed from well before staining, they will be regarded as viable cells because of non-specific staining by crystal violet [37]. The generalised protocol is that, macrophages are washed with PBS and incubated with 0.2% (w/v) crystal violet containing 2% (v/v) ethanol in PBS at 37 °C for 30 min. Finally, macrophages are washed with PBS and the crystal violet is solubilized with 33% (v/v) acetic acid in water.

Absorbance at 540 nm is measured in a microplate reader [50].

5.8. Cell cycle analysis

Macrophage cells (1×10^6 cells/ml) are seeded in 6-well plates and exposed to stimuli. After treatment, cells are washed in PBS and collected. They are then fixed in 70% glacial ethanol, washed in PBS, resuspended in 1 ml of PBS containing 50 U/ml RNase and 50 μg/ml propidium iodide (PI) and then incubated in dark for 40 min at 4 °C. Cell cycle analysis is performed by flow cytometry and the population of cells in various phases are calculated [51].

6. Morphological observation

After encountering stimuli, macrophages are induced to undergo morphodynamics such as increase in cell size, production of thin sheets of cell edges called filopodia (contains actin filaments) or lamellopodia (bears actin spikes) [21]. Change in morphological contour hence represents a clear indication of macrophage functionality activation or repression.

6.1. Bright field light microscopy

Cells are seeded on round glass coverslips at a density of 2×10^5 cells/well in 24-well plate. Following treatment with a stimulus, the supernatant is discarded and replaced with 4% paraformaldehyde fixative (300 μl/well). The plate is incubated at 8 °C for 2 h, wells are washed thoroughly with PBS (300 μl/well) to remove fixative and adherent cells are serially dehydrated in an ethanol series at 70, 80, 90 and 95% (5 min each bath). For cell staining, Harris hematoxylin (300 μl/well) is added for 1 min and the excess stain is removed by washing the coverslips with distilled water. Afterwards, 300 μl/well aqueous eosin is added for 30 s and rinsed. The glass coverslips are allowed to dry, mounted with Entellan on clean slide and analysed under bright field microscope [52].

6.2. Fluorescence microscopy

Macrophage cells are cultured in presence of sample on cover slides in 12-well plate or directly in 6-well plate for definite period of time. After incubation, cells are washed with PBS and incubated with DAPI (4′,6-diamidino-2-phenylindole) (1 μg/ml in PBS) for 15 min [20,21,53]. The cells may also be stained with $DiOC_6$ (3,3′-dihexyloxacarbocyanine iodide) along with DAPI as shown in Supplementary Fig. 2. Alternatively, cells are fixed in 4% (v/v) paraformaldehyde for 15 min and stained with DAPI (300 nmol/l) for 30 min at RT. Then cellular and nuclear morphology can be visualized, examined, and photographed by fluorescence microscopy [54].

6.3. Scanning electron microscopy (SEM) or transmission electron microscopy (TEM)

Treated and untreated macrophages are cultured on 6-well plate or glass coverslips in 24-well plates. After incubation, cells are washed with PBS, fixed overnight with 2–2.5% glutaraldehyde in 0.1 M cacodylate buffer and followed by post fixation with 1% osmium tetroxide for 2 h. Subsequently, the fixed cells are dehydrated through a graded series of alcohol and dried under a Critical Point Dryer. Further the cells are sputter-coated with gold. The morphological changes can be observed under an electron microscope and photographed [55].

7. Determination of phagocytic uptake

The term phagocytosis is used to define the cellular engulfment of particles larger than 0.5 μm in diameter. In immune response, the first and imperative defence function of macrophages is represented by phagocytosis that causes ingestion as well as elimination of pathogenic or inflammatory particles [56]. At first, antigens are recognized directly by pathogen-associated molecular patterns (PAMPs) by pattern-recognition receptor (PRR) of innate immune system or indirectly by a process called opsonisation [57]. After PRR engagement, the foreign particles are internalized via protrusions of cell membrane forming a vesicle called phagosome. These phagosomes are transported within cytosol and its content becomes gradually acidified. After complete maturation, phagosome fuses with lysosome that bears a range of hydrolytic enzymes and anti-microbial peptides. This highly oxidative and acidic environment causes oxidative burst and subsequent elimination of its contents by exocytosis [58]. Thus, increase in phagocytic activity can definitely help to boost immunity and also signals for macrophage stimulation. Currently, there are a number of methods available to assess *in vitro* phagocytic activity. Most of these techniques use latex minibeads (0.75 mm), zymosan, *Escherichia coli* or yeast particles and some of these components are available in market labelled with fluorescein isothiocyanate (FITC).

7.1. Zymosan particles

Zymosan is an insoluble β-1,3-glucan polysaccharide, extracted from *Saccharomyces cerevisiae* and has been widely used for more than 50 years as a perfect model for microbial particle in studies on immune response. Since the preparation contains PAMP, they are easily recognized by innate immune recognition receptors stimulating phagocytosis and inflammatory cytokine production [59]. To perform the assay, macrophages are cultured in 24-well plate containing glass coverslips (13 mm diameter). After treatment with sample, they are allowed to phagocytose zymosan (1×10^6 particles/well) for 1 h at 37 °C. The cells are washed with PBS to remove non-digested particles, coverslips are fixed with 4% paraformaldehyde, stained with May-Grünwald reagent or Wright's stain [50]. The engulfment power can be investigated microscopically by counting individual cells and calculating average number of particles internalized per 100/200 macrophages for each experimental treatment. Phagocytic index (PI) is used to express overall effect and determined by using the following formula [60]:

PI = Percentage phagocytosis × mean number of particles per cell

7.2. Killed yeast cells

Commercial baker's yeast (10–30 mg) is mixed in 10 ml PBS and heat-killed (80 °C for 15 min). Hundred μl of yeast cell suspension (around 1×10^8 cells/ml) are flooded onto macrophage cells on slide or 24-well plate. After incubation at 37 °C for 1.5–2 h, the cells are washed thrice with PBS to remove non-phagocytosed cells and air dried. Finally, macrophages are fixed in 100% methanol, stained with Giemsa dye or 0.1% crystal violet for 3–5 min (Supplementary Fig. 3). Cells are dried and counted without any predetermined pattern to calculate phagocytosis percentage and phagocytic index [61].

Phagocytosis percentage (P%) = Macrophages showing phagocytosis/ Total no. of macrophages × 100%

Phagocytic index (PI) = Total no. of yeast cells phagocytosed/ macrophages showing phagocytosis × P%

7.3. Live bacterial cells

After treatment, supernatant is removed and macrophage cells, cultured in 24-well plate, are flooded with 100 μl of freshly prepared *E. coli* cell suspension (2×10^6 cells/ml) and incubated at 37 °C. After

90 min, each well is washed to remove non-phagocytosed bacterial cells. Then cells can be lysed with 0.1% SDS and the lysates are plated on agar. After overnight incubation at 37 °C, colonies are counted [61].

7.4. FITC labelled particles

Cells are cultured in 6-well plate or 35 mm dish or on glass coverslips in 24-well plate. After incubation, treated medium is replaced with 1 ml PBS containing 100 μl FITC labelled beads (diameter: 2 μm) and incubated at 37 °C for 30 min to 2 h in dark. Finally, the adherent cells are washed thrice with PBS, fixed with paraformaldehyde (4% in PBS) for 30 min or 100 μl of 10% Triton X-100 and finally excess beads are removed by washing. Phagocytosis can also be stopped by repeated washing with cold PBS. Otherwise, the cells can be centrifuged for 5 min at 400×*g* at RT. The supernatant is removed and the cells are washed two times with 1 ml of PBS. Finally, cells are suspended in 500 μl of PBS and immediately analysed by flow cytometer [62].

8. Determination of pinocytic activity by neutral red assay

Pinocytosis is another type of endocytotic process by which macrophages take up fluid from surrounding medium along with molecules contained in it. To detect the potentiality, macrophages are seeded in 96-well plate at 2×10^4 cells/well and after 6 h, incubated with stimuli. Following treatment, 100 μl of 0.075%–0.1% neutral red prepared in 10 mM PBS or culture medium is added in each well. The reaction is incubated for one–two h followed by washing cells by PBS for three times to remove residual natural red solution. Then, 100–200 μl of cell lysis buffer (1:1 of ethanol:acetic acid v/v or ethanol: 1 mol/l acetic acid = 1:1 or 1% glacial acetic acid:ethanol = 1:1 or 1% acetic acid solution: 50% ethanol = 1:1) is added in each well and the mixture is incubated at RT for 4 h or overnight. Absorbance is read at 540 nm using ELISA plate reader. Pinocytic activity is expressed as pinocytic index and calculated as described in NBT assay at the phagocytosis section [20,56,63].

9. Intracellular calcium assay

Calcium ion is a ubiquitous second messenger that controls multiple processes in immune cells, including chemotaxis, adhesion, and secretion of pro- and anti-inflammatory cytokines. Resting cells have a Ca^{2+} concentration around 100 nM which may quickly reach up to 1 μM when cells are stimulated [38]. Release of Ca^{2+} from endoplasmic reticulum (ER) activates store-operated Ca^{2+} entry channels in plasma and/or phagosomal membrane, leading to elevations in cytosolic Ca^{2+} concentration. The phenomenon helps in efficient ingestion of foreign particles by some phagocytic receptors, controls subsequent steps involved in maturation of phagosome, solubilisation of surrounding actin meshwork, fusion of phagosomes with granules containing lytic enzymes and activation of superoxide generating NADPH oxidase complex [64]. This elevated level of cytosolic calcium, in turn, triggers transcription factors (TFs) such as activator protein-1 (AP-1; a heterodimeric protein constituted of c-Fos and c-Jun) and signal transducer and activator of transcription (STAT)1, STAT3; subsequently increasing transcription of pro-inflammatory target genes [65]. The change in intracellular Ca^{2+} concentration signifies activation state of macrophages which can be detected by using certain stains.

9.1. Fluo-4 dye

Fluo-4 ($C_{36}H_{30}F_2N_2O_{13}$) is a dynamic single-wavelength fluorescent Ca^{2+} indicator and an increase in fluorescence intensity reflects a rise in the cytoplasmic Ca^{2+} level [66]. To execute the technique, macrophage cells are seeded in 96-well plates and after treatment the media is removed. Then, cells are incubated with 100 μl of dye loading solution for 30 min and fluorescence intensity is determined spectrofluorometrically with excitation and emission filters of 485 nm and 535 nm respectively [65].

9.2. Fura-2 dye

Fura-2 ($C_{44}H_{47}N_3O_{24}$) represents another fluorescent Ca^{2+} indicator that is widely used to monitor cytoplasmic Ca^{2+} levels. Upon Ca^{2+} binding, the fluorescence excitation spectrum is shifted toward shorter wavelength. Usually, the intensity of fluorescence induced by 340 nm and 380 nm excitation and emitted at 510 nm is measured, and therefore Fura-2 is a ratiometric dye that minimizes effects of photobleaching, leakage and uneven loading. The ratio of F340/F380 fluorescence intensity is proportional to the cytoplasmic Ca^{2+} level [66]. The generalised protocol is that, after treatment macrophages are incubated with 5 μM of Fura-2 for 45 min at 37 °C. They are then washed twice with Hank's Balanced Salt Solution (HBSS) buffer (pH 7.2). Ratiometric calcium imaging is performed with an inverted fluorescence microscope [67].

10. Measurement of NO production

Nitric oxide is a membrane-permeable inorganic gas as well as free radical. It is synthesized from L-arginine by nitric oxide synthase and released by macrophages in response to pathogens. Therefore, increase in NO production is considered as an indication of macrophage activation [68]. However, this gaseous molecule is extremely short lived and rapidly oxidized to nitrate and/or nitrite by oxygen. Thus, measurement of stable and non-volatile breakdown product of NO like nitrite (NO_2^-) is the best-known mean to investigate NO formation [69].

10.1. Griess reagent (iNtRON)

In Griess reaction, established in 1879, NO_2^- is first treated with sulphanilamide, a diazotizing agent, in acidic environment to form a diazonium salt. This transient intermediate is then allowed to react with N-[1-napnthyl]-ethylenediamide dihydrochloride (NED) to generate purple coloured stable azo compound [69]. To perform the assay, macrophage cells in 96-well plates (1×10^5 cells/well) or 24-well plates (3×10^5 cells/well) are pre-incubated for 12 h. Following treatment, 100 μl of Griess reagent (1% w/v sulphanilamide, 0.1% w/v NED in 5% phosphoric acid) is mixed with 100 μl of culture supernatant. The mixture is incubated at RT for 15 min and optical density is measured spectrophotometrically at 540 nm. The nitrite concentration is calculated from a standard curve derived from a reaction with sodium nitrite (0–100 μM) [40].

10.2. DAF2-DA

The assay is a fluorescence-based method that uses a cell permanent 4,5-diaminofluorescein diacetate (DAF2-DA) as NO detector. Diacetate (DA) part of the dye is hydrolysed in presence of cellular esterases to produce DAF2 compound that reacts with NO to produce a fluorescent triazolofluorescein (DAF-2T). To follow the assay, cells are seeded on coverslips in 6-well plates overnight and then treated with sample for desired time. Thereafter, cells are stained with 10 μM/ml DAF2-DA for 20–30 min at RT, washed with PBS and then fluorescence intensity is recorded at ex/em 480/535 nm [70].

11. Analysis of ROS production

The term ROS describes a group of molecules with at least one oxygen atom and with higher reactivity than O_2 [71]. They play an important role for antimicrobial activity of macrophages. In fact after pathogen recognition and phagocytosis, cytosolic subunits of NADPH oxidase (NOX) are phosphorylated and migrate to the phagosome membrane to form a functional enzyme with membrane-bound subunits. Following NADPH oxidase assembling, formation of superoxide radical

($O_2^{\bullet-}$) takes place inside the phagosome for up to 2 h approximately and the phenomenon is called oxidative burst. Eventually NO is produced in the cytosol of macrophages and readily diffuses across phagosome membrane due to its hydrophobic nature [72]. Nitric oxide then reacts with superoxide anion resulting in reactive nitrogen species (RNS) including peroxynitrite ($ONOO^-$). These oxidants induce nitrosative stress that promotes ROS production and are capable to kill microorganisms [73]. Release of ROS by the inflammatory cells can be quantified by various methods such as electron spin resonance spectroscopy, spectrophotometric measurements and chemiluminescence.

11.1. L-012

L-012, (8-amino-5-chloro-7-phenylpyrido [3,4-d]pyridazine-1,4 (2H,3H)dione) is a luminol-derivative chemiluminescence probe and highly sensitive for ROS. To carry out an assay for ROS detection, culture supernatant of treated and untreated macrophage cells is removed and replaced by an equal volume of HBSS supplemented with 25 μM L-012 and 5 μg/ml horseradish peroxidase (HRP) with or without PMA. Reactions are monitored on a Fluoroscan microtiter plate reader at 37 °C. Chemiluminescence is measured every 2 min for 2 h and is expressed as the integrated response over the time [49].

11.2. DCHFDA

The fluorogenic probe 2′,7′-dichlorofluorescein-diacetate (DCHFDA) is able to diffuse into cell and deacetylated by cellular esterase. The resulting product is a non-fluorescent compound which is then oxidized by ROS into 2′,7′-dichlorofluorescein (DCF). The resulting compound is highly fluorescent; hence can be detected by fluorescence spectroscopy [18]. To perform the assay, cells are washed with DMEM after treatment and stained with 10 μM of DCFDA at 37 °C for 20 min. Cells are washed with PBS twice and the fluorescence intensities can be measured at 485/20 nm excitation wavelength and 528/20 nm emission wavelength using a multimode microplate reader [74] or flow cytometry [20].

11.3. CM-DCFH

Intracellular ROS can also be measured by detecting the fluorescent intensity of carboxyl-2′,7′-dichlorofluorescein diacetate (CM-DCFH) oxidized product, CM-DCF. After treatment, cells are harvested and washed with cold PBS. Washed cells are further incubated with 10 mM CM-DCFH at RT for 30 min. Relative fluorescent intensity of the fluorophore can be detected at ex/em 485/530 nm or using a fluorescence microscope [75].

11.4. Dihydrorhodamine123

Dihydrorhodamine 123 is a nonfluorescent and uncharged ROS indicator that can diffuse passively across membranes. The molecule in presence of ROS is oxidized to cationic rhodamine 123 which is trapped in mitochondria and exhibits green fluorescence [76]. The dihydrorhodamine123 is added to each well (10 μM/well) containing treated or untreated macrophage cells and incubated for 15–30 min at RT. The fluorescent intensity is analysed by spectrofluorometer with excitation and emission wavelengths of 485/15 and 535/10 nm respectively [65].

11.5. Reduction of NBT

Macrophage cells (2×10^5 cells/ml) are plated on 96-well plates and cultured with sample. The cells are further incubated with 200 μl of PBS containing 0.1% of nitro-blue tetrazolium (NBT) and 2 μg/ml PMA at 37 °C for 30 min. This membrane permeable, water-soluble, yellow-coloured NBT reacts with superoxide anion produced inside phagocytic cells and is reduced to blue coloured formazan. The reaction is terminated with 80 μl of 70% methanol and cells are dried. The blue formazan produced is then dissolved in 2 M KOH (120 μl) and DMSO (140 μl) and absorbance is measured by a spectrophotometer at 620/10 nm against KOH/DMSO [77].

12. Measurement of H_2O_2 production

Hydrogen peroxide (H_2O_2), a primary component of ROS, is an uncharged, stable and freely diffusible second messenger. The agent is commonly produced from superoxide by superoxide dismutase (SOD) 1 and 2 during oxidative stress generated in phagocytic cells [73]. While superoxide crosses cell membrane poorly, H_2O_2 diffuses easily between extra- and intracellular environments. Indeed, H_2O_2 diffuses into bacterial cytoplasm and potentially causes damage of a variety of molecules [78]. Intracellular H_2O_2 is also capable of triggering downstream signal pathways inducing pro-inflammatory cytokines production [79]. Generally, the treated and untreated macrophages are subjected to 100 μl of phenol red buffer containing peroxidase (5 mM glucose, 0·56 mM phenol red solution and 8·5 UI/ml HRP). Following incubation for 1 h at 37 °C, the reaction is stopped by addition of 10 μl of 1 M NaOH. Absorbance is then determined at 620 nm using a microplate reader. The concentration of H_2O_2 is determined based on the standard curve for H_2O_2 [80].

13. Acid phosphatase activity/cellular lysosomal enzyme activity

During phagocytosis, macrophage cells acquire acid phosphatase by fusion with lysosomes. Thus, acid phosphatase functions as a signal enzyme for macrophage activation. To investigate the activity, treated cell supernatant is thoroughly removed and 25 μl of Triton X-100 (1%) along with 150 μl of *p*-nitrophenyl phosphate solution (1 mg/ml) are added. The mixtures are incubated for 1 h and 50 μl of NaOH solution (3 M) is added to terminate the reaction. Finally, absorbance is detected at 405 nm. The index of acid phosphatase activity is obtained according to the following equation [56]:

Index of acid phosphatase activity = Absorbance of treatment/Absorbance of blank

14. Recognition of membrane receptors

To eradicate pathogens, macrophages must be able to distinguish between self-particles and infectious materials. The molecules mainly responsible for making this pivotal distinction are those of family of transmembrane glycol-protein receptors called TLRs. These receptors were named after the fruit-fly receptor Toll, which was recognized as contributing to innate immunity in adult flies [81]. To date, total 13 mammalian TLRs have been recognized, of which 12 functional TLRs (TLR1–TLR9, TLR11–TLR13) have been identified to be expressed in mice and 10 (TLR1–TLR10) in humans where TLRs 1–9 are conserved in both. Typically TLRs 1, 2, 4–6 and 10 are displayed in cell surface and the rest are localized to intracellular compartments such as ER, endosome, lysosome, or endolysosome. Cell surface TLRs recognize mainly microbial membrane components including lipoproteins, lipids and proteins [82]. Activation of TLR-4 results in triggering two dissimilar cascades such as myeloid differentiating primary response gene 88 (MyD88) dependent and MyD88 independent pathway. Stimulation of MyD88 led to generation of pro-inflammatory cytokines via triggering of a TF, NF-κB, (Fig. 2). Stimulation MyD88-independent pathway, on the other hand, led to synthesis of type 1 interferons (IFN)s [83]. Apart from TLRs, macrophages also contain mannose receptor (MR) that binds to microbial structure bearing mannose, N-acetylglucosamine and fucose on surface triggering endocytosis and phagocytosis [84]. Dectin-1 is another PRR that is expressed on macrophage surface and recognizes

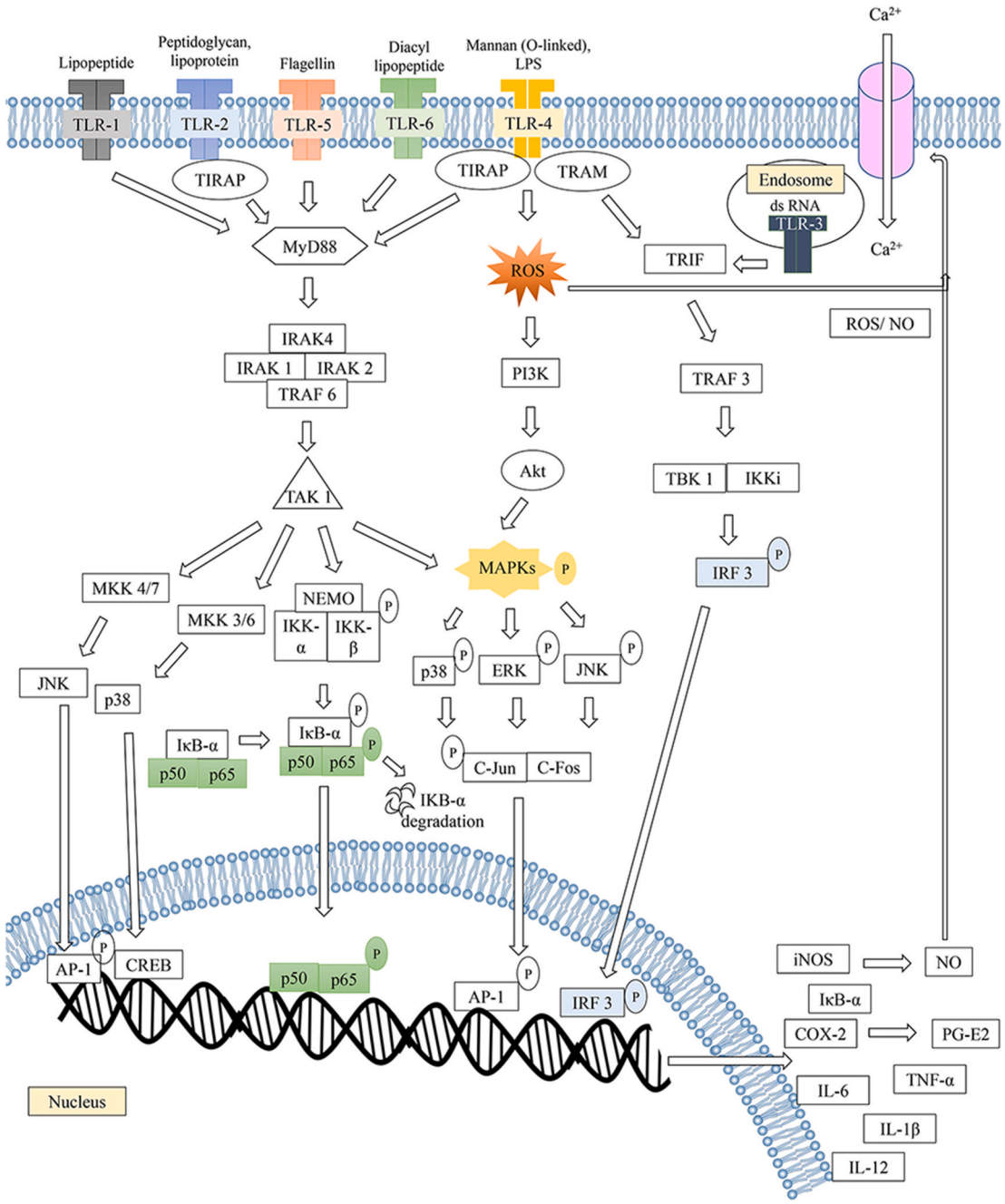

Fig. 2. Schematic representation of TLRs pathway in macrophage cells based on previous studies [15,17,44,70,82].

β-glucans in cell walls of fungi. Activation of the receptor results in phagocytosis, ROS production, synthesis of inflammatory cytokines and chemokines that in turn influences development of adaptive immunity [85]. Several other receptors such as scavenger receptor (SR), glucocorticoid receptor (GR) and complement receptor 3 (CR3) also play an important role in inflammation, innate immunity and host defence. To detect the involved receptor, polymerase chain reaction (PCR), western blotting and RNA interference (RNAi) techniques are the most prevalent methods.

14.1. RNA isolation, cDNA preparation, reverse transcriptase-PCR

After treatment, macrophage cells are lysed by 1 ml TRIzol reagent. Then 200 μl chloroform is added, lysates are shaken vigorously by hand for 15 s and incubated at RT for 2–3 min. After centrifugation for 15 min, the aqueous phase is transferred to a fresh tube. RNA is washed thoroughly with isopropyl alcohol and 75% ethanol. The pellet is briefly dried and dissolved in RNase-free water. Total RNA yield is measured by 260 nm absorbance and its quality can be assessed by agarose gel electrophoresis [86]. Reverse transcription of RNA is carried out using reverse transcriptase, oligo (dT) 16 primer, dNTP and RNase inhibitor. The generated cDNA is amplified by PCR using primer set for specific gene (Table 2 and Table 3) where β-actin or GAPDH are used as housekeeping genes. The cDNA is generally amplified by 35 cycles of denaturing at 94 °C for 45 s, annealing for 45 s, extension at 72 °C for 1 min and finally extended at 72 °C for 5 min. The products can be separated in 1.5% (w/v) agarose gels and visualized with UV light [393]. For each gel, ImageJ software (http://rsbweb.nih.gov/ij/index.html) might be applied for quantitative estimation of band intensity.

Table 2
List of mouse specific primers to test immunomodulatory activity.

Gene	Primer sequences	Tm (°C)	References
TLR-2	F: 5′ AGCATCCGAATTGCATCACC 3′ R: 5′ ACCCCAGAAGCATCACATGA 3′	55	[86]
	F: 5′ CACCACTGCCCGTAGATGAAG 3′ R: 5′ AGGGTACAGTCGTCGAACTCT 3′	NM	[75]
	F: 5′ GGGGCTTCACTTCTCTGCTT 3′ R: 5′ AGCATCCTCTGAGATTTGACG 3′	NM	[87]
TLR-3	F: 5′ GATACAGGGATTGCACCCATA 3′ R: 5′ TCCCCCAAAGGAGTACATTAGA 3′	NM	[87]
TLR-4	F: 5′ TGTATTCCCTCAGCACTCTT 3′ R: 5′ GCATCATAGATGCTTTCTCC 3′	NM	[88]
	F: 5′ CGCTCTGGCATCATCTTCAT 3′ R: 5′ GTTGCCGTTTCTTGTTCTTCC 3′	NM	[89]
	F: 5′ GGTGTGAAATTGAGACAATTGAAAAC 3′ R: 5′ GTTTCCTGTCAGTACCAAGGTTGA 3′	NM	[90]
	F: 5′ TTGCTGCCAACATCATCCAG 3′ R: 5′ GGTCCAAGTTGCCGTTTCTT 3′	55	[86]
	F: 5′ CAGCTTCAATGGTGCCATCA 3′ R: 5′ CTGCAATCAAGAGTGCTGAG 3′	NM	[91]
	F: 5′ GCCTTTCAGGGAATTAAGCTCC 3′ R: 5′ GATCAACCGATGGACGTGAAA 3′	NM	[73]
	F: 5′ GGACTCTGATCATGGCACTG 3′ R: 5′ CTGATCCATGCATTGGTAGGT 3′	NM	[87]
Dectin-1	F: 5′ ACAGTACACCAGACACAGGG 3′ R: 5′ TGGCCAGACAGCATAAGGAA 3′	NM	[86]
CR3	F: 5′ CCATGACCTTCCAAGAGAATGC 3′ R: 5′ ACCGGCTTGTGCTGTAGTC 3′	NM	[73]
MYD88	F: 5′ GCCAGAGTGGAAAGCAGTGT 3′ R: 5′ CGTTGGGGCAGTAGCAGATA 3′	55	[17]
	F: 5′ TGGCCTTGTTAGACCGTGA 3′ R: 5′ AAGTATTTCTGGCAGTCCTCCTC 3′	NM	[87]
TRIF	F: 5′ TGGCAAACACCTTCAAGACA 3′ R: 5′ GCGCTTTCTTCCAGCGTA 3′	NM	[87]
NF-κB	F: 5′ ATGGCAGACGATGATCCCTAC 3′ R: 5′ CGGAATCGAAATCCCCTCTGTT 3′	NM	[92]
	F: 5′ CAGACGATGATCCCTACGGAA 3′ R: 5′ TCCCCTCTGTTTTGGTTGCT 3′	60	[93]
	F: 5′ AGAAGGCTGGGGTCAATCTT 3′ R: 5′ CTCAGGCTTTGTAGCCAAGG 3′	NM	[90]
IRG1	F: 5′ GCTTTTGTTAATGGTGTTGCTG 3′ R: 5′ GGCTTCCGATAGAGCTGTGA 3′	NM	[87]
iNOS	F: 5′ AGGGACTGAGCTGTTAGAGACA 3′ R: 5′ AAGAGAAACTTCCAGGGGCAAG 3′	55	[94]
	F: 5′ CTGCAGCACTTGGATCAGGAACCTG 3′ R: 5′ GGGAGTAGCCTGTGTGCACCTGGAA 3′	57	[44,95,96]
	F: 5′ CCCTTCCGAAGTTTCTGGCAGCAGC 3′ R: 5′ GGCTGTCAGAGCCTCGTGGCTTTGG 3′	56–60	[97]
	F: 5′ CGGCAAACATGACTTCAGGC 3′ R: 5′ GCACATCAAAGCGGCCATAG 3′	NM	[9,98]
	F: 5′ CATGCTACTGGAGGTGGGTG 3′ R: 5′ CATTGATCTCCGTGACAGCC 3′	NM	[99,100]
	F: 5′ TTCCAGAATCCCTGGACAAG 3′ R: 5′ TGGTCAAACTCTTGGGGTTC 3′	NM	[89]
	F: 5′ TTGTGCATCGACCTAGGCTGGAA 3′ R: 5′ GACCTTTCGCATTAGCATGGAAGC 3′	NM	[88]
	F: 5′ GGTAGTAGTAGAATGGAGATAGG 3′ R: 5′ CTACCTAAGATAGCAGTTGATG 3′	NM	[76]
	F: 5′ ATGGCTTGCCCCTGGAA 3′ R: 5′ TATTGTTGGGCTGAGAA 3′	NM	[92]
	F: 5′ TCCCTTCCGAAGTTTCTGGC 3′ R: 5′ CTCTCTTGCGGACCATCTCC 3′	NM	[101]
	F: 5′ CCTCCTCCACCCTACCAAGT 3′ R: 5′ CACCCAAAGTGCTTCAGTCA 3′	60	[102]
	F: 5′ GCCCTGCTTTGTGCGAAGTGTCAG 3′ R: 5′ GCACCTGGAACAGCACTCTCTTG 3′	NM	[90]
	F: 5′ GAGCGAGTTGTGGATTGTC 3′ R: 5′ GGAGGAGCTGATGGAGT 3′	55	[15,103]
	F: 5′ AATGGCAACATCAGGTCGGCCATCACT 3′ R: 5′ GCTGTGTGTCACAGAAGTCTCGAACTC 3′	NM	[104]
	F: 5′ CACCTTGGAGTTCACCCAGT 3′ R: 5′ ACCACTCGTACTTGGGATGC 3′	NM	[73]

Table 2 (*continued*)

Gene	Primer sequences	Tm (°C)	References
	F: 5′ ACGCTGAGTACCTCATTGGC 3′ R: 5′ AGCTCCTCCCAGGACCACAC 3′	62	[46,104]
	F: 5′ CTGGGACAGCACAGAATG 3′ R: 5′ GCCTTGTGGTGAAGAGTGTC 3′	55	[51]
	F: 5′ GAGCGAGTTGTGGATTGTC 3′ R: 5′ CCAGGAAGTAGGTGAGGG 3′	55	[105]
	F: 5′ CAACCAGTATTATGGCTCCT 3′ R: 5′ GTGACAGCCCGGTCTTTCCA 3′	55	[106]
	F: 5′ GTCTTGCAAGCTGATGGTCA 3′ R: 5′ GGCCTCAGCTTCTCATTCTG 3′	52	[107]
	F: 5′ CAAATCCTACCAAGTGACCTGAAAGAG 3′ R: 5′ GGTTCCTGTTGTTTCTATTTCCTTTGTTAC 3′	56	[40]
	F: 5′ GTGCTGCCTCTGGTCTTGCAAGC 3′ R: 5′ AGGGGCAGGCTGGGAATTCG 3′	55–60	[108]
	F: 5′ CCCTCCTGATCTTGTGTTGGA 3′ R: 5′ TCAACCCGAGCTCCTGGAA 3′	NM	[87]
	F: 5′ TGGGAATGGAGACTGTCCCAG 3′ R: 5′ GGGATCTGAATGTGATGTTTG 3′	NM	[91]
TNF-α	F: 5′ ACCTGGCCTCTCTACCTTGT 3′ R: 5′ CCCGTAGGGCGATTACAGTC 3′	55	[94]
	F: 5′ ATGAGCACAGAAAGCATGATC 3′ R: 5′ TACAGGCTTGTCACTCGAATT 3′	56	[20,89,95]
	F: 5′ GGGGATTATGGCTCAGGGTC 3′ R: 5′ CGAGGCTCCAGTGAATTCGG 3′	NM	[9,98]
	F: 5′ AGTTCTATGGCCCAGACCCTC 3′ R: 5′ GCTACAGGCTTGTCACTCGAA 3′	60	[93]
	F: 5' TGGAACTGGCAGAAGAGGCA 3' R: 5' TGCTCCTCCACTTGGTGGTT 3'	NM	[88]
	F: 5′ AGTGACAAGCCTGTAGCC 3′ R: 5′ AGGTTGACTTTCTCCTGG 3′	NM	[109]
	F: 5′ CACGCTCTTCTGTCTACTG 3′ R: 5′ ACTTGGTGGTTTGCTAC 3′	NM	[76]
	F: 5′ CATCCTCTCAAAATTCGAGTGACA 3′ R: 5′ TGGGAGTAGACAAGGTACAACCC 3′	NM	[110]
	F: 5′ AGCCCCCAGTCTGTATCCTT 3′ R: 5′ CTCCCTTTGCAGAACTCAGG 3′	NM	[111]
	F: 5′ CAGGCGGTGCCTATGTCTC 3′ R: 5′ CGATCACCCCGAAGTTCAGTAG 3′	NM	[92]
	F: 5′ ATAGCTCCCAGAAAAGCAAGC 3′ R: 5′ CACCCCGAAGTTCAGTAGACA 3′	NM	[99]
	F: 5′ GAACTGGCAGAAGAGGCACT 3′ R: 5′ AGGGTCTGGGCCATAGAACT 3′	NM	[101]
	F: 5′ GTGGAACTGGCAGAAGAGGC 3′ R: 5′ AGACAGAAGAGCGTGGTGGC 3′	60	[102]
	F: 5′ ACTTCGGGGTGATCGGTC 3′ R: 5′ TGTCTTTGAGATCCATGCCG 3′	60	[112]
	F: 5′ TGCCTATGTCTCAGCCTCTTC 3′ R: 5′ GAGGCCATTTGGGAACTTCT 3′	55	[113]
	F: 5′ AGCACAGAAAGCATGATCCG 3′ R: 5′ CCTGATGAGAGGGAGGCCATT 3′	NM	[73]
	F: 5′ ACAAGCCTGTAGCCCACG 3′ R: 5′ TCCAAAGTAGACCTGCCC 3′	NM	[104]
	F: 5′ CACCCTTATTCTCGCTCAC 3′ R: 5′ CCCGCTTACAGTTCCTCT 3′	53	[105]
	F: 5′ GGACTAGCCAGGAGGGAGAA 3′ R: 5′ CGCGGATCATGCTTTCTGTG 3′	55	[51]
	S: 5′ TGAGGCTGGATAAGATCTCAG 3′ A: 5′ CAGAGGTTCAGTGATGTAGCG 3′	60	[39,114]
	F: 5′ GGGCTACAGGCTTGTCACTCG 3′ R: 5′ ACTCCAGGCGGTGCCTATGTC 3′	NM	[90]
	F: 5′ AGCACAGAAAGCATGATCCG 3′ R: 5′ CTGATGAGAGGGAGGCCATT 3′	NM	[100]
	F: 5′ CCTGTAGCCCACGTCGTAGC 3′ R: 5′ TTGACCTCAGCGCTGAGTTG 3′	55	[96]
	F: 5′ ATCAGTTCTATGGCCCAGAC 3′ R: 5′ AGGAGGTTGACTTTCTCCTG 3′	54	[40]
	F: 5′ TTGACCTCAGCGCTGAGTTG 3′ R: 5′ CCTGTAGCCCACGTCGTAGC 3′	55–62	[46,97]
	F: 5′ CGGGATCCATGAGCACAGAAAGCAT 3′ R: 5′ CCCAAGCTTTCACAGAGCAATGACTCC 3′	NM	[85]
		NM	[91]

(*continued on next page*)

Table 2 (*continued*)

Gene	Primer sequences	Tm (°C)	References
	F: 5′ AACTTCGGGGTGATCGGTCC 3′ R: 5′ CAAATCGGCTGACGGTGTGGG 3′		
COX-2	F: 5′ CCACTTCAAGGGAGTCTGGA 3′ R: 5′ AGTCATCTGCTACGGGAGGA 3′	60	[115]
	F: 5′ CCCCCACAGTCAAAGACACT 3′ R: 5′ GAGTCCATGTTCCAGGAGGA 3′	57	[20,100]
	F: 5′ GTACTGGCTCATGCTGGACGA 3′ R: 5′ CACCATACACTGCCAGGTCAGCAA 3′	NM	[88]
	F: 5′ GGTGCCTGGTCTGATGATG 3′ R: 5′ TGCTGGTTTGGAATAGTTGCT 3′	NM	[92]
	F: 5′ TCTGGAACATTGTGAACAACATC 3′ R: 5′ AAGCTCCTTATTTCCCTTCACAC 3′	NM	[99]
	F: 5′ AGAAGGAAATGGCTGCAGAA 3′ R: 5′ GCTCGGCTTCCAGTATTGAG 3′	NM	[89]
	F: 5′ AGGAGACATCCTGATCCTGGT 3′ R: 5′ GTTCAGCCTGGCAAGTCTTT 3′	60	[102]
	F: 5′ CACTACATCCTGACCCACTT 3′ R: 5′ ATGCTCCTGCTTGAGTATGT 3′	55	[113]
	F: 5′ CCCCCACAGTCAAAGACACT 3′ R: 5′ CTCATCACCCCACTCAGGAT 3′	NM	[104]
	F: 5′ TCTCAGCACCCACCCGCTCA 3′ R: 5′ GCCCCGTAGACCCTGCTCGA 3′	55–60	[108]
	F: 5′ TGGTGCCTGGTCTGATGATG 3′ R: 5′ GTGGTAACCGCTCAGGTGTTG 3′	NM	[87]
	F: 5′ TGGACGAGGTTTTTCCACCAG 3′ R: 5′ CAAAGGCCTCCATTGACCAGA 3′	NM	[116]
	F: 5′ TGATCGAAGACTACGTGCAAC 3′ R: 5′ GCCAAAGTTGTCATGGATG 3′	NM	[117]
IFN-α	F: 5′ CCTGTGTGATGCAGGAACC 3′ R: 5′ TCACCTCCCAGGCACAGA 3′	NM	[99]
IFN-β	F: 5′ ACTAGAGGAAAAGCAAGAGGA 3′ R: 5′ CTGGTAAGTCTTCGAATGATG 3′	NM	[99]
IFN-γ	F: 5′ GATGCTCTTCGACCTCGAAACAGCAT 3′ R: 5′ ATGAAATATACAAGTTATAATCTTGGCTTT 3′	NM	[95]
	F: 5′ CTCAAGTGGCATAGATGT 3′ R: 5′ GAGATAATCTGGCTCTGCAGGATT 3′	NM	[89]
	F: 5′ CCTCAAACTTGGCAATACTCA 3′ R: 5′ CTCAAGTGGCATAGATGTGGA 3′	NM	[90]
	F: 5′ CCAAGTTTGAGGTCAACAAC 3′ R: 5′ CTTATTGGGACAATCTCTTCC 3′	55	[49]
IL-1β	F: 5′ GCCACCTTTTGACAGTGATGAG 3′ R: 5′ AGTGATACTGCCTGCCTGAAG 3′	55	[94]
	F: 5′ AAGGAGCTATCACTTGACCAC 3′ F: 5′ CTTCATCTTTTGGGGTCCGTC 3′	60	[93]
	F: 5′ ATGGCAACTATTCCAGAACTCAACT 3′ R: 5′ CAGGACAGGTATAGATTCTTTCCTTT 3′	NM	[95]
	F: 5′ GGCAGGCAGTATCACTCATT 3′ R: 5′ CCCAAGGCCACAGGTATTT 3′	NM	[88]
	F: 5′ ATCTCGCAGCAGCACATC 3′ R: 5′ CCAGCAGGTTATCATCATCATC 3′	NM	[76]
	F: 5′ AAATACCTGTGGCCTTG 3′ R: 5′ TTAGGAAGACACGGATTC 3′	NM	[109]
	F: 5′ AAGGGCTGCTTCCAAAC 3′ R: 5′ CTCCACAGCCACAATGA 3′	NM	[92]
	F: 5′ ACCTGCTGGTGTGTGACGTT 3′ R: 5′ TCGTTGCTTGGTTCTCCTTG 3′	NM	[99]
	F: 5′ CCTTGGGCCTCAAAGGAAAGAATC 3′ R: 5′ GGAAGACACAGATTCCATGGTGAAG 3′	NM	[101]
	F: 5′ GGGCCTCAAAGGAAAGAATC 3′ R: 5′ TACCAGTTGGGGAACTCTGC 3′	NM	[89]
	F: 5′ AAGGAGACCAAGCAACGACAAAA 3′ R: 5′ TGGGGACTCTGCAGACTCAAACT 3′	NM	[111]
	F: 5′ CCTCGTGCTGTCGGACCCAT 3′ R: 5′ CAGGCTTGTGCTCTGCTTGTGA 3′	57–60	[99,105]
	F: 5′ GAGCTTCAGGCAGGCAGTAT 3′ F: 5′ TGGGTGTGCCGTCTTTCATT 3′	60	[111]
	F: 5′ ATGGCAACTGTTCCAGAACTCAACT 3′ R: 5′ CAGGACAGGTATAGATTCTTTCCTTT 3′	NM	[44]
		NM	[104]

Table 2 (*continued*)

Gene	Primer sequences	Tm (°C)	References
	F: 5′ ATGGCAACTGTTCCTGAACTCAACT 3′ R: 5′ GTGCTGCCTAATGTCCCCTTGAATC 3′		
	F: 5′ TGCAGAGTTCCCCAACTGGTACATC 3′ R: 5′ GTGCTGCCTAATGTCCCCTTGAATC 3′	55	[96]
	F: 5′ TGCTTCCAAACCTTTGACCTGGGC 3′ R: 5′ CAGGGTGGGTGTGCCGTCTTTC 3′	NM	[108]
	F: 5′ AAGAAGAGCCCATCCTCTGT 3′ R: 5′ CGCTTTTCCATCTTCTTCTT 3′	55	[40]
	F: 5′ CAAGGAGAACCAAGCAAC 3′ R: 5′ GGGGAAGGCATTAGAAAC 3′	60	[39,114]
	F: 5′ TACAAGGAGAACCAAGCAACGACA 3′ R: 5′ TGTCGTTGCTTGGTTCTCCTTGTA 3′	NM	[91]
IL-6	F: 5′ TACTCGGCAAACCTAGTGCG 3′ R: 5′ GTGTCCCAACATTCATATTGTCAGT 3′	NM	[9,98]
	F: 5′ CAACGATGATGCACTTGCAGA 3′ R: 5′ TCTCTCTGAAGGACTCTGGCT 3′	55	[94]
	F: 5′ TTCCTCTCTGCAAGAGACT 3′ R: 5′ TGTATCTCTCTGAAGGACT 3′	56	[20,44,95]
	F: 5′ GTCGGAGGCTTAATTACACA 3′ R: 5′ TTCATACAATCAGAATTGCCAT 3′	60	[96]
	F: 5′ GAGGATACCACTCCCAACAGACC 3′ R: 5′ AAGTGCATCATCGTTGTTCATACA 3′	NM	[88]
	F: 5′ AATTAAGCCTCCGACTTGTG 3′ R: 5′ CACGCTCTTCTGTCTACTG 3′	NM	[76]
	F: 5′ CCGGAGAGGAGACTTCACAG 3′ R: 5′ GGAAATTGGGGTAGGAAGGA 3′	NM	[110]
	F: 5′ GGAGTACCATAGCTACCTGG 3′ R: 5′ CTAGGTTTGCCGAGTAGATC 3′	NM	[109]
	F: 5′ ATGAAGTTCCTCTCTGCAA 3′ R: 5′ AGTGGTATCCTCTGTGAAG 3′	NM	[92]
	F: 5′ TGGAGTCACAGAAGGAGTGGCTAAG 3′ R: 5′ TCTGACCACAGTGAGGAATGTCCAC 3′	NM	[99]
	F: 5′ TCCATCCAGTTGCCTTCTTG 3′ R: 5′ GGTCTGTTGGGAGTGGTATC 3′	NM	[101]
	F: 5′ AGTTGCCTTCTTGGGACTGA 3′ R: 5′ CAGAATTGCCATTGCACAAC 3′	NM	[89]
	F: 5′ CACTTCACAAGTCGGAGGC 3′ R: 5′ GCACTAGGTTTGCCGAGTAGA 3′	60	[112]
	F: 5′ CCGGAGAGGAGACTTCACAG 3′ R: 5′ CAGAATTGCCATTGCACAAC 3′	60	[102]
	F: 5′ GGAGTACCATAGCTACCTGG 3′ R: 5′ CTAGGTTTGCCGAGTAGATC 3′	NM	[90]
	F: 5′ GTACTCCAGAAGACCAGAGG 3′ R: 5′ TGCTGGTGACAACCACGGCC 3′	NM	[46,104]
	F: 5′ AGTTGCCTTCTTGGGACTGA 3′ R: 5′ CAGAATTGCCATTGCACAAC 3′	NM	[104]
	F: 5′ TTCCTCTCTGCAAGAGACTTC 3′ R: 5′ GGTCTGTTGGGAGTGGTATC 3′	55	[51]
	F: 5′ TGCACTTGCAGAAAACAATC 3′ R: 5′ TTAGGAGAGCATTGGAAATTG 3′	54	[40]
	F: 5′ GCTGGAGTCACAGAAGGAGTGGC 3′ R: 5′ GGCATAACGCACTAGGTTTGCCG 3′	55–60	[108]
	F: 5′ TGAACAACGATGATGCACTT 3′ R: 5′ CGAAGAGAACAACATAAGTC 3′	NM	[39]
	F: 5′ ATGAAGTTCCTCTCTGCAAG 3′ R: 5′ GGTTTGCCGAGTACATCTCA 3′	NM	[85]
	F: 5′ GCCAGAGTCCTTCAGAGAGAGATACAG 3′ R: 5′ CCCAACATTCATATTGTCAG 3′	NM	[91]
IL-10	F: 5′ TGGCCCAGAAATCAAGGAGC 3′ R: 5′ CAGCAGACTCAATACACACT 3′	60	[115]
	F: 5′ TACCTGGTAGAAGTGATGCC 3′ R: 5′ CATCATGTATGCTTCTATGC 3′	NM	[44]
	F: 5′ CCAAGCCTTATCGGAAATGA 3′ R: 5′ TTTTCACAGGGGAGAAATCG 3′	NM	[92]
	F: 5′ GTGAAGACTTTCTTTCAAACAAAG 3′ R: 5′ CTGCTCCACTGCCTTGCTCTTATT 3′	NM	[99]
IL-12	F: 5′ CCACAAAGGAGGCGAGACTC 3′ R: 5′ CTCTACGAGGAACGCACCTT 3′	NM	[44,95]
	F: 5′ AACCAGACCCGCCCAAGAAC 3′ R: 5′ GATCCTGAGCTTGCACGCAGA 3′	NM	[88]
IL-12p35	F: 5′ TCAGCGTTCCAACAGCCTC 3′ R: 5′ CGCAGAGTCTCGCCATTATG 3′	55	[39]
		55	[114]

(*continued on next page*)

Table 2 (*continued*)

Gene	Primer sequences	Tm (°C)	References
	F: 5′ CTGCATCAGCTCATCGATGG 3′ R: 5′ CAGAAGCTAACCATCTCCTGGTTT 3′		
IL-12p40	F: 5′ CAGAAGCTAACCATCTCCTGGTTT 3′ R: 5′ TCCGGAGTAATTTGGTGCTTCACAC 3′	55	[39,97]
	F: 5′ TCCGGAGTAATTTGGTGCTTCACA 3′ R: 5′ ACTGTACAACCGCAGTAATACGG 3′	55	[114]
IL-18	F: 5′ ACTGTACAACCGCAGTAATACGG 3′ R: 5′ AGTGAACATTACAGATTTATCCC 3′	58	[39]
	F: 5′ TGAACAACGATGATGCACTT 3′ R: 5′ CGTAGAGAACAACATAAGTC 3′	58	[114]
MKP-1	F: 5′ GCATCCCTGTGGAGGACAACC 3′ R: 5′ TCCAGCATCCTTGATGGAGTCTATG 3′	55	[118]
MIP-2	F: 5′ GAACAAAGGCAAGGCTAACTGA 3′ R: 5′ AACATAACAACATCTGGGCAAT 3′	NM	[99]
MCP-1	F: 5′ ACTGAAGCCAGCTCTCTCTTCCTC 3′ R: 5′ TTCCTTCTTGGGGTCAGCACAGAC 3′	NM	[99]
	F: 5′ GGAAAAATGGATCCACACCTTGC 3′ R: 5′ TCTCTTCCTCCACCACCATGCAG 3′	NM	[88]
NOX-2	F: 5′ ACCAGACAGACTTGAGAATG 3′ R: 5′ GCTGTGCTATGTTGCTCTAG 3′	NM	[76]
CCL3	F: 5′ TGCCCTTGCTGTTCTTCTCT 3′ R: 5′ GTGGAATCTTCCGGCTGTAG 3′	NM	[87]
PTGIS	F: 5′ CAGACGACCACTCTCCCACAG 3′ R: 5′ GGAAGAGGAGGAGGCGGT 3′	60	[115]
Granzyme-B	F: 5′ AGATCGAAAGTGCGAATCTGA 3′ R: 5′ TTCGTCCATAGGAGACAATGC 3′	NM	[95]
Perforin	F: 5′ AGTCCTCCACCTCGTTGTCCGTGA 3′ R: 5′ AAAGTCAGCTCCACTGAAGCTGTG 3′	NM	[95]
NKG2D	F: 5′ GACTTCACCAGTTTAAGTAAATC 3′ R: 5′ CTGGGAGATGAGTGAATTTCATA 3′	NM	[95]
FasL	F: 5′ CCAGAGAGAGCTCAGATACGTTGAC 3′ R: 5′ ATGTTTCAGCTCTTCCACCTACAGA 3′	NM	[95]
GPR120	F: 5′ GATGACAATGAGCGGCAGCG 3′ R: 5′ GATTTCTCCTATGCGGTTGGG 3′	NM	[89]
GM-CSF	F: 5′ ACTCTGCTCACGAAGGAACTCAGC 3′ R: 5′ CACAGCTCGGAAGAGCATCGCA 3′	NM	[108]
LY96	F: 5′ AATACCATTCTCTTTCGAGG 3′ R: 5′ CTTTTCTTCAGTATCCCCA 3′	60	[93]
18s rRNA	F: 5′ TCGAGGCCCTGTAATTGGAA 3′ R: 5′ CCCTCCAATGGATCCTCGTT 3′	NM	[92]
	F: 5′ CGCTCGCTCCTCTCCTACT 3′ R: 5′ ATCGGCCCGAGGTTATCTA 3′	55	[40]
β-actin	F: 5′ CGCCACCAGTTCGCCATGGA 3′ R: 5′ TACAGCCCGGGGAGCATCGT 3′	60	[115]
	F: 5′ TGGAATCCTGTGGCATCCATGAAAC 3′ R: 5′ TAAAACGCAGCTCAGTAACAGTCCG 3′	55–60	[39,96,100,114]
	F: 5′ CATCTCTTGCTCGAAGTCCA 3′ R: 5′ ATCATGTTTGAGACCTTCAACA 3′	NM	[95]
	F: 5′ GCTGTGCTATGTTGCTCTAG 3′ R: 5′ TCGTTGCCAATAGTGATGAC 3′	NM	[76]
	F: 5′ TCACCCACACTGTGCCCATCTACGA 3′ R: 5′ GGATGCCACAGGATTCCATACCCA 3′	NM	[99]
	F: 5′ CCACAGCTGAGAGGGAAATC 3′ R: 5′ AAGGAAGGCTGGAAAAGAGC 3′	NM	[89]
	F: 5′ AGCCATGTACGTAGCCATCC 3′ R: 5′ CTCTCAGCTGTGGTGGTGAA 3′	NM	[73,111]
	F: 5′ ATCACTATTGGCAACGAGCG 3′ R: 5′ TCAGCAATGCCTGGGTACAT 3′	NM	[100,101]
	F: 5′ CCCTGTATGCCTCTGGTCGT 3′ R: 5′ CACCAGACAGCACTGTCTTGG 3′	60	[112]
	F: 5′ GCTGTCCCTGTATGCCTCT 3′ R: 5′ TTGATGTCACGCACGATTT 3′	55	[20,103]
	F: 5′ GACGTTGACATCCGTAAAG 3′ R: 5′ CAGTAACAGTCCGCCT 3′	NM	[104]
	F: 5′ GTGGGCCGCCCTAGGCACCAG 3′ R: 5′ GGAGGAAGAGGATGCGGCAGT 3′	62	[46,104,108]
	F: 5′ AACTGGAACGGTGAAGGTGA 3′ R: 5′ GTGCAATCAAAGTCCTCGGC 3′	55	[49]
	F: 5′ AGGCATCCTGACCCTGAAGTAC 3′ R: 5′ TTCATGAGGTAGTCTGTCAG 3′	52	[107]
	F: 5′ GGAGAAGATCTGGCACCACACC 3′ R: 5′ CCTGCTTGCTGATCCACATCTGCTGG 3′	55	[106]
	F: 5′ AACCGTGAAAAGATGACCCAGAT 3′ R: 5′ CACAGCCTGGATGGCTACGT 3′	NM	[87]

Table 2 (*continued*)

Gene	Primer sequences	Tm (°C)	References
	F: 5′ GGACAGTGAGGCCAGGATGG 3′ R: 5′ AGTGTGACGTTGACATCCGTAAAGA 3′	NM	[116]
GAPDH	F: 5′ GGTGAAGGTCGGTGTGAACG 3′ R: 5′ CCCGTAGGGCGATTACAGTC 3′	55	[94]
	F: 5′ GGACTGTGGTCATGAGCCCTTCCA 3′ R: 5′ ACTCACGGCAAATTCAACGGCAC 3′	NM	[88]
	F: 5′ AACGGATTTGGCCGTATTGG 3′ R: 5′ CTTCCCGTTCAGCTCTGGG 3′	NM	[109]
	F: 5′ ACCAGAGTCCATGCCATCAC 3′ R: 5′ CACCACCCTGTTGCTGTAGCC 3′	NM	[110]
	F: 5′ AGAGTGTTTCCTCGTCCCGTA 3′ R: 5′ AAATCCGTTCACACCGACCT 3′	60	[93]
	F: 5′ TGTGTCCGTCGTGGATCTGA 3′ R: 5′ TTGCTGTTGAAGTCGCAGGAG 3′	60	[102]
	F: 5′ ACAACTTTGGCATTGTGGAA 3′ R: 5′ GATGCAGGGATGATGTTCTG 3′	NM	[90]
	F: 5′ TTTGTCAAGCTCATTTCCTGGTATG 3′ R: 5′ TGGGATAGGGCCTCTCTTGC 3′	NM	[9,98]
	F: 5′ AACAGCAACTCCCACTCTTC 3′ R: 5′ CCTGTTGCTGTAGCCGTATT 3′	NM	[73]
	F: 5′ CTCTGCTCCTCCCTGTTC 3′ R: 5′ CAATCTCCACTTTGCCACT 3′	52	[105]
	F: 5′ CACTCACGGCAAATTCAACGGCAC 3′ R: 5′ GACTCCACGACATACTCAGCAC 3′	60	[97]
	F: 5′ TGTGATGGGTGTGAACCACGAG 3′ R: 5′ TGCTGTTGAAGTCGCAGGAGAC 3′	NM	[91]

NM: Not mentioned.

14.2. Quantitative PCR (qPCR)

Quantitative PCR relies on real-time detection of amplified cDNA targets generated by successive rounds of PCR. Amplicons are detected based on fluorescence intensity which increases uniformly with the PCR product. However, the required equipment and reagents are more expensive than that of conventional PCR technology. To perform the assay, cDNA is prepared from each experimental set as described before and then amplified by using incorporation of SYBR green. Relative expression of specific genes can be calculated using $2^{-\Delta\Delta}$CT method [9,17,18,40,74,99,101,105].

14.3. Receptor detection by inhibitor treatment

Cells are adjusted to a concentration of 1×10^6 cells/ml in the exponential phase, loaded into 96-well plate (100 μl/well) and incubated for 24 h. Cells are pre-treated with TLR4-IN-C34, a drug that inhibits TLR-4, for 30 min, followed by incubation with sample. After the incubation period, cell supernatant is analysed for NO content by using Griess reagent [17]. Otherwise, the cells can be pre-treated with antibodies (5 μg/ml) of membrane receptors (SR, MR, GR, CR3, TLR-2, TLR-4 and Dectin-1) for 1–2 h to blockade the matched receptors. Then, above cells are cultured with sample at 37 °C in humidified chamber. The cells treated with sample in absence of antibody and the cells without any treatment are used as control groups. Then the activities of treated macrophages can be determined in terms of NO production in culture supernatant [9,63,99].

14.4. Western blot analysis

One of the disadvantages of transcriptome analysis is that presence of mRNA does not always precisely reflect protein level as many proteins are modified at post-translational level. The limitation can be overcome by performing western blotting method. For that, macrophage cells are grown in 6-well plate (1×10^6 cells/well) with stimuli or other treatment. Cells are lysed using cell lysis buffer (100–300 μl/well) prepared by mixing 20 mM 4-(2-hydroxyethyl)-1-piperazineethanesulfonic acid (HEPES) (pH 7.4), 2 mM ethylene glycol-bis(β-aminoethyl ether)-N,N,

Table 3
List of human specific primers to test immunomodulatory activity.

Gene	Primer sequences	Tm (°C)	References
NF-κB	F: 5′ GGTGCGGCTCATGTTTACAG 3′	60	[118]
	R: 5′ GATGGCGTCTGATACCACGG 3′		
IL-1β	F: 5′ TGATGGCTTATTACAGTGGCAATG 3′	60	[119]
	R: 5′ GTAGTGGTGGTCGGAGATTCG 3′		
	F: 5′ GGCTTATTACAGTGGCAATG 3′	60	[120]
	R: 5′ TAGTGGTGGTCGGAGATT 3′		
	F: 5′ GGGATAACGAGGCTTATGTGC 3′	NM	[121]
	R: 5′ AGGTGGAGAGCTTTCAGTTCA 3′		
	F: 5′ CCCTCTGTCATTCGCTCCC 3′	NM	[122]
	R: 5′ CACTGCTACTTCTTGCCCCC 3′		
IL-4	F: 5′ TCTTTGCTGCCTCCAAGAAC 3′	60	[118]
	R: 5′ GCGAGTGTCCTTCTCATGGT 3′		
IL-6	F: 5′ CCAGCCTGCTGACGAAGC 3′	60	[118]
	R: 5′ TCAGGCTGGACTGCAGGAAC 3′		
	F: 5′ CACACAGACAGCCACTCACC 3′	60	[119]
	R: 5′ GCTCTGGCTTGTTCCTCACT 3′		
IL-8	F: 5′ ACCACCGGAAGGAACCATCTC 3′	60	[118]
	R: 5′ AGCTGCAGAAATCAGGAAGGC 3′		
IL-10	F: 5′ TTTAAGGGTTACCTGGGTTGC 3′	60	[118]
	R: 5′ CCTTGATGTCTGGGTCTTGG 3′		
IFN-α	F: 5′ CAGCCTGGATAACAGGAGGA 3′	60	[118]
	R: 5′ CTCCTGGGGAAATCCAAAGT 3′		
TGF-β	F: 5′ CACTTCATCAACCCGGAAAC 3′	60	[118]
	R: 5′ AGGATGACGTTGGAGCTGTC 3′		
TNF-α	F: 5′ CCCGACTATCTCGACTTTGC 3′	60	[118]
	R: 5′ AAGGTTGGATGTTCGTCCTC 3′		
	F: 5′ CGAGTCTGGGCAGGTCTA 3′	NM	[122]
	R: 5′ GTGGTGGTCTTGTTGCTTAA 3′		
	F: 5′ TGAGCACTGAAAGCATGATCC 3′	NM	[121]
	R: 5′ GGAGAAGAGGCTGAGGAACA 3′		
	F: 5′ ATGAGCACTGAAAGCATGATCC 3′	60	[119]
	R: 5′ GAGGGCTGATTAGAGAGAGGTC 3′		
CSF-1	F: 5′ GGAGACCTCGTGCCAAATTA 3′	60	[119]
	R: 5′ GGCCTTGTCATGCTCTTCAT 3′		
CYP1A1	F: 5′ TCCTGGAGCCTCATGTATT 3′	61	[120]
	R: 5′ TCTCTTGTTGTGCTGTGG 3′		
18srRNA	F: 5′ CAGCCACCCGAGATTGAGCA 3′	61	[120]
	R: 5′ TAGTAGCGACGGGCGGTGTG 3′		
β-actin	F: 5′ CACTCTTCCAGCCTTCCTTCC 3′	60	[118]
	R: 5′ GCACTGTGTTGGCGTACAGG 3′		
	F: 5′ CACCATTGGCAATGA GCGGTTC 3′	NM	[121]
	R: 5′ AGGTCTTTGCGGATGTCCACGT 3′		
GAPDH	F: 5′ GGTGGTCTCCTCTGACTTCAACAG 3′	60	[119]
	R: 5′ GTTGCTGTAGCCAAATTCGTTGT 3′		
	F: 5′ GGAGCGAGATCCCTCCAAAAT 3′	NM	[122]
	R: 5′ GGCTGTTGTCATACTTCTCATGG 3′		

NM: Not mentioned.

N′,N’-tetraacetic acid (EGTA), 50 mM glycerophosphate, 1 mM sodium orthovanadate, 1% Triton X-100, 10% glycerol, and protease inhibitor. Else, RIPA (radioimmunoprecipitation assay) buffer [50 mM Tris-Cl (pH 8.0), 5 mM EDTA, 150 mM NaCl, 1% NP-40, 0.1% SDS and 1 mM phenylmethylsulfonyl fluoride] can also be used. The supernatant is collected after centrifugation at 13,200×*g* for 20 min and can be assayed for protein content using bovine serum albumin (BSA) as a standard. After heat denaturation for 7 min, aliquots containing 40 μg of protein are separated on 8–16% (w/v) Tris/glycine/sodium dodecyl sulfate polyacrylamide (SDS-PAGE) gel. The separated proteins are then transferred to polyvinylidene difluoride (PVDF) membrane which is then blocked with 5% non-fat dry milk in Tris-buffered saline/Tween (TBS-T) (137 mM NaCl, 20 mM Tris-HCl (pH 7.4) and 0.1% Tween 20). The blots are then incubated with diluted primary antibody at 4 °C. Subsequently, the membrane is washed five times and incubated with an appropriate secondary antibody (HRP-conjugated goat anti-mouse or anti-rabbit IgG) (1:500) in 2% (v/v) PBS for 1–2 h. After washing the membrane with TBST three times for 10 min, the blots can be developed with chemiluminescence [95,123].

14.5. RNAi

RNA interference involves double-stranded RNA-mediated degradation of target mRNA. Such gene-specific suppression can be achieved by delivering of 21–23 nucleotide long interfering RNAs (siRNAs) [124]. To determine whether the mechanism of action of the investigating drug is mediated through TLR-4, MyD88 or TRIF, the mRNAs can be silenced using oligonucleotide sequences as described by Qi and Shelhamer [123]. The siRNA duplexes are transfected into macrophage cells which are then seeded at 0.2×10^6 cell/well in 24-well plate. After 24 h of transfection, the medium is changed with 1 ml of fresh DMEM and treated with stimuli. For RNA and protein extraction, the cells are harvested in TRIzol after 6 h and 12 h of treatment respectively [88]. The interference of TLR4, MyD88, and TRIF protein expression can be confirmed by immunoblotting using specific antibodies [123].

15. Assays on NF-κB protein

Nuclear factor kappa-B is a key pro-inflammatory TF that regulates transcription of numerous regulatory receptors, cytokines, chemokines and enzymes. The protein is activated when macrophages sense pathogens through multiple classes of PRR pathways [125]. The protein consists of homo- and hetero-dimers of five subunits, p65/RelA, RelB, c-Rel, p50/NF-κB1 and p52/NF-κB2. In resting cells, NF-κB localizes in cytoplasm via association with cytosolic IκB (inhibitor of NF-κB) proteins such as IκB-α, -β and -ε. Upon stimulation, IκB kinase (IKK) phosphorylates IκB which is then degraded by ubiquitin-proteasome system [126]. Subsequently, NF-κB dimer then translocates to nucleus, binds to its consensus sequence on promoter and enhancer of target genes and activates transcription of pro-inflammatory genes (Fig. 2). Monitoring NF-κB movement hence is a widespread method to measure activity of the TF. Two techniques have been developed to test the translocation: 1) Cell fractionation isolating cytoplasmic and nuclear fractions where NF-κB is quantified using anti-phospho–NF–κB p65 by western blotting [95]. 2) Image-based tracking of NF-κB where dynamics of the protein are monitored either by antibody staining or using a fluorescent protein fused to the TF [126,127].

15.1. Immunofluorescence study to visualize NF-κB nuclear localization

Immunofluorescence assay (IFA) is a microscopic technique to detect and visualize any protein expressed in cells via antigen-antibody reaction. To perform the assay, treated macrophage cells, grown on glass cover slips, are fixed with 4% paraformaldehyde in PBS for 15–20 min at RT. Cells are then repeatedly washed with PBS (5 min each) and permeabilized with 0.3–2% Triton X-100 in PBS for 5 min. Cells are again washed and then blocked with 1–5% BSA in PBS for 1 h. Cells are then incubated with primary antibodies against NF-κB p65 (1:200 or 1:400) overnight at 4 °C. After washing three times, cells are incubated with appropriate secondary antibodies (1:500) of fluorescent dye-conjugated anti-rabbit IgG or fluorescent dye conjugated goat anti-rabbit IgG plus 10 μg/ml of Hoechst 33342 for 1–2 h at RT in dark. Cells are then washed three times with PBS and DAPI (1 μg/ml in PBS) is used to stain nuclei. Finally, sample on cover slips may be mounted with non-hardening, aqueous-based compound, available commercially, to provide a semi-permanent seal for storage of slide preparations. The observations can be performed on a fluorescence microscope with 100 × magnification capturing micrographs [128].

15.2. Inhibition of NF-κB using specific inhibitors

BAY 11–7082 (BAY) is an inhibitor of NF-κB and thus used to verify action of the TF mediated signalling pathway. Research has established that BAY strongly suppresses production of NO, prostaglandin E2 (PGE2), and tumor necrosis factor-α (TNF-α). It also reduces the translocation of p65 and its upstream signalling events such as

phosphorylation of IκB-α, IKK, and Akt [129]. Thus, to investigate the signal transduction pathway, macrophage cells are incubated with BAY (1 μM) for 2 h. The monocytes are then treated with sample for definite period of time. Afterwards, TNF-α content in the culture supernatant is determined using ELISA technique [63].

15.3. Transient transfection and luciferase reporter assay

Macrophage cells are cultured in a 60-mm dish. After confluence, they are transfected with pNF-κB-Luc plasmid comprising NF-κB responsive region followed by receptor gene firefly luciferase along with certain antibiotic resistant gene. After 48 h, cells are cultured in medium supplemented with the antibiotic for at least one week. Clone revealing the strongest luciferase activity due to LPS treatment is seeded (4×10^5 cells/well) in 24-well plate for overnight. After treatment with drug, cells are harvested and extracted with lysis buffer (100 μl). Twenty μl of the lysate is then mixed with 100 μl luciferin and the luminescence is measured. Results can be described as relative luciferase activity (fold difference in comparison with negative control) [75,92,114,128].

15.4. Electrophoretic mobility shift assay (EMSA)

Electrophoretic mobility shift assay is classically used to detect DNA binding proteins. Principle of the technique is that protein-DNA complex moves more slowly through a polyacrylamide gel than the corresponding free linear unbound DNA. This high sensitivity and simple to perform method can be used for studying DNA and protein interactions [130]. The assay traditionally requires radioactive probes; however, biotin or fluorescent probes are now available. To perform the assay, treated and untreated macrophage cells are centrifuged at 800×*g* for 5–10 min at 4 °C. Cells are lysed with 300 μl pre-cold hypotonic buffer (5 μl phosphatase inhibitor, 10 μl phenylmethylsulfonyl fluoride (PMSF) and 1 μl dithiothreitol or DTT in 1 ml of buffer). The tube is flicked with finger, bathed on ice for 10 min and shaken for 10 s. The suspension is centrifuged at 800×*g* for 5 min and the supernatant is discarded immediately. The buffer (400 μl) is added to wash the pellet and the tubes are again centrifuged at 2,500×*g* for 5 min. The supernatant is discarded and the precipitate is saved. Lysis buffer (200 μl) (10 μl PMSF, 5 μl phosphatase inhibitor and 1 μl DTT in 1 ml buffer) is added to the precipitate, bathed on ice for 20 min and centrifuged at 20,000×*g* for 10 min or 14,500×*g* for 15 min. Precipitate is discarded and the supernatant is stored at −80 °C as nuclear protein extract. The protein concentration can be measured using BSA. NF-κB or p65 (5′AGTTGAGGGGACTTTCCCAGGC3′) probe is labelled with biotin or [$^{\gamma}$-32P]-ATP. NF-κB probe (0.5 μl) and nuclear protein extract (40 μg protein) are incubated in binding reaction for 20 min at RT. Non-denaturing 6.5% PAGE is carried out and electrotransfer is carried out in TBE buffer. Gel is dried and subjected to autoradiography or chemiluminescence [23,95].

15.5. RelA translocation assay

In order to interpret NF-κB activation, a nuclear translocation assay can be performed. The method is based on quantification of the amount of translocated p65 subunit or RelA in nucleus and comparison with that of remaining in the cytoplasm. Accordingly, treated and untreated macrophages are fractionated into nuclear and cytoplasmic fractions, supernatants are collected separately and p65 is quantified in each by Western blot technique [131].

16. Determination of cytokines and chemokines expression

Cytokines are a diverse group of low molecular weight protein that act as pro- or anti-inflammatory factors at pico or nanomolar levels to regulate inflammation and cellular activities. Whilst, inflammatory chemokines are generated in response to an inflammatory stimulus and facilitate an immune response. Binding of a cytokine or chemokine ligand triggers a cascade of events regulating various cellular functions such as phagocytosis, cytokine secretion, cell activation and cell proliferation, among others. These potent signalling molecules thus are a cornerstone of any investigation that deals with inflammation [132]. Following macrophage activation, NF-κB promotes gene expression of a wide variety of cytokines such as interleukin (IL)-1β, IL-2, IL-6, IL-12, TNF-α and granulocyte-macrophage colony-stimulating factor (GM-CSF); chemokines such as IL-8, macrophage inflammatory proteins (MIP)-1, monocyte chemoattractant protein-1 (MCP-1) or C–C motif chemokine ligand (CCL)2, regulated on activation normal T cell expressed and secreted (RANTES) or CCL5 and eotaxin; and inducible effector enzymes such as inducible nitric oxide synthase (iNOS) and cyclooxygenase-2 (COX-2) (Fig. 2) [133]. NF-κB activates its own inhibitor, IκB-α, as well which then translocates to the nucleus, binds to promoter bound NF-κB, and returns it to cytoplasm in an inactivate state. Such post-induction repression process eventually terminates transcription [134]. Overall, NF-κB serves as a 'rapid acting' primary TF which can regulate host's early innate immune response to infection and also associated with chronic inflammatory states and multiorgan failure [133]. Several methods have been developed to measure cytokine levels; amongst them ELISA is routinely used.

16.1. Quantitative analysis by ELISA

The procedure exploits specificity of antibodies and uses them to quantify an analyte of interest with remarkable sensitivity. To perform the method, macrophage cells are seeded into 6 or 12-well plates (1×10^6 cells/well). After treatment, culture media are transferred into 96-well plates coated with 100 μl of antibody solutions of cytokines at 37 °C for 1 h. Following four washes, 100 μl of HRP solution is added and the plates are left to stand for 40 min. The solution is washed repeatedly and 3,3′,5,5′-tetramethylbenzidine (TMB) substrate solution (100 μl) is added. The reaction mixtures are incubated in the dark and a stop solution is added after 15 min. After 5 min, the absorbance is read at 450 nm on a microplate reader. The cytokine levels are computed according to standard curves and generally represented in picograms per milliliter [127].

16.2. Other methods

Protein levels of IκB-α, *p*-IκBα (Ser32), STAT3, p-STAT3 (Tyr705), iNOS, COX-2, phosphor(p)-ERK1/2, SAPK/JNK, TNF-α, IL-1, IL-6, P38, p-p38, ERK1/2, JNK, *p*-JNK, α-Tubulin, c-jun, c-fos and β-actin expression can be measured by Western blotting [89,135–137]. Expression of DNA binding proteins such as p38, SAPK/JNK, c-src, AP-1, Ras and Akt can be detected by EMSA as described above [79].

17. Evaluation of expression of co-stimulatory molecules

Macrophage cells play an important role as an interface between innate and adaptive immunity. Following activation, the cells express markers (CD68, CD86, CD80, F4/80, CD11b, CD40, B7-1 and B7-2) known as co-stimulatory molecules that are responsible for functions such as antigen processing and presentation to antigen-specific T cells. CD40 interacts with CD40L, which is known to play key roles in activation and differentiation of B cells. Thus, increase in expression of these surface molecules indicates enhanced immune response [95,138].

To perform the assay, cells are collected following treatment and then washed with PBS. The cell surfaces are blocked with 5% goat serum for 15 min or staining buffer comprising 10% normal mouse serum for 20 min on ice and washed twice. Subsequently, the cells are incubated with monoclonal antibodies against CD80, CD40, CD86 and corresponding fluorescent markers for around 30 min at 4 °C. Following washing, the cells are fixed by 1% paraformaldehyde in PBS. The fixed cells are subjected to flow cytometry and minimum 5000 cells are

analysed for each sample [95].

18. cDNA microarray

cDNA microarray technology leads to identification of specific genes and allows researchers to compare profiles of gene expression in normal versus pathological conditions [139]. In brief, macrophage cells are placed at a density of 5×10^5 cells/ml in medium and treated with stimuli. The total RNA is extracted from each treatment and utilized for cDNA synthesis, labelling and microarray hybridization. The resulting localized concentrations of fluorescent molecules are noticed and quantitated [54].

19. Conclusion and future prospects

In recent years, immunotherapy has become of great interest to researchers, clinicians and pharmaceutical companies as it has the high potential to revolutionize treatment regimens. In that note, *in vitro* assays have shown their usefulness as an initial platform for drug development elucidating mode of action. However, techniques related to transcriptome analysis, estimation of protein expression and detection of post-translational modification are comparatively expensive, hindering many researchers to perform the assays. Thus, attempt should be taken to standardize more cost-effective and easier to perform procedures to make way wider and smoother for testing and discovering novel therapeutic agents.

CRediT authorship contribution statement

Somanjana Khatua: performed the literature search, wrote the manuscript. **Jesus Simal-Gandara:** conceived the idea and revised the manuscript. **Krishnendu Acharya:** conceived the idea and revised the manuscript.

Declaration of competing interest

The authors declare that they have no known competing financial interests or personal relationships that could have appeared to influence the work reported in this paper.

Acknowledgements

Funding for open access charge: Universidade de Vigo/CISUG.

Appendix A. Supplementary data

Supplementary data to this article can be found online at https://doi.org/10.1016/j.cbi.2021.109776.

References

[1] A.A. Khan, K.N. Manzoor, A. Sultan, M. Saeed, M. Rafique, S. Noushad, A. Talib, S. Rentschler, H.P. Deigner, Pulling the brakes on fast and furious multiple drug-resistant (MDR) bacteria, Int. J. Mol. Sci. 22 (2021) 859, https://doi.org/10.3390/ijms22020859.
[2] L.M. Pezzanite, L. Chow, V. Johnson, G.M. Griffenhagen, L. Goodrich, S. Dow, Toll-like receptor activation of equine mesenchymal stromal cells to enhance antibacterial activity and immunomodulatory cytokine secretion, Vet. Surg. 50 (2021) 858–871, https://doi.org/10.1111/vsu.13628.
[3] P. Saroj, M. Verma, K.K. Jha, M. Pal, An overview on immunomodulation, J. Adv. Sci. Res. 3 (2012) 7–12.
[4] K. Singh, A. Rao, Probiotics: a potential immunomodulator in COVID-19 infection management, Nutr. Res. 87 (2021) 1–12, https://doi.org/10.1016/j.nutres.2020.12.014.
[5] M. Mrityunjaya, V. Pavithra, R. Neelam, P. Janhavi, P.M. Halami, P.V. Ravindra, Immune-boosting, antioxidant and anti-inflammatory food supplements targeting pathogenesis of COVID-19, Front. Immunol. 11 (2020), 570122, https://doi.org/10.3389/fimmu.2020.570122.
[6] C. Lee, W.J. Choi, Overview of COVID-19 inflammatory pathogenesis from the therapeutic perspective, Arch Pharm. Res. (Seoul) 44 (2021) 99–116, https://doi.org/10.1007/s12272-020-01301-7.
[7] C.K. Ong, P. Lirk, C.H. Tan, R.A. Seymour, An evidence-based update on nonsteroidal anti-inflammatory drugs, Clin. Med. Res. 5 (2007) 19–34, https://doi.org/10.3121/cmr.2007.698.
[8] D. Kumar, V. Arya, R. Kaur, Z.A. Bhat, V.K. Gupta, V. Kumar, A review of immunomodulators in the Indian traditional health care system, J. Microbiol. Immunol. Infect. 45 (2012) 165–184, https://doi.org/10.1016/j.jmii.2011.09.030.
[9] L. Jiang, G. Zhang, Y. Li, G. Shi, M. Li, Potential application of plant-based functional foods in the development of immune boosters, Front. Pharmacol. 12 (2021), 637782, https://doi.org/10.3389/fphar.2021.637782.
[10] H.A.E. Enshasy, R. Hatti-Kaul, Mushroom immunomodulators: unique molecules with unlimited applications, Trends Biotechnol. 31 (2013) 668–677, https://doi.org/10.1016/j.tibtech.2013.09.003.
[11] S. Beg, S. Swain, H. Hasan, M.A. Barkat, M.S. Hussain, Systematic review of herbals as potential anti-inflammatory agents: recent advances, current clinical status and future perspectives, Phcog. Rev. 5 (2011) 120–137, https://doi.org/10.4103/0973-7847.91102.
[12] P.K. Sarkar, C. Das Mukhopadhyay, Ayurvedic metal nanoparticles could be novel antiviral agents against SARS-CoV-2, Int. Nano Lett. 11 (2021) 197–203, https://doi.org/10.1007/s40089-020-00323-9.
[13] H. Sakagami, K. Kishino, O. Amano, Y. Kanda, S. Kunii, Y. Yokote, H. Oizumi, T. Oizumi, Cell death induced by nutritional starvation in mouse macrophage-like RAW264.7 Cells, Anticancer Res. 29 (2009) 343–348.
[14] J. Lam, M. Herant, M. Dembo, V. Heinrich, Baseline mechanical characterization of J774 macrophages, Biophys. J. 96 (2009) 248–254, https://doi.org/10.1529/biophysj.108.139154.
[15] S. Khatua, S. Paloi, K. Acharya, An untold story of a new myco-resource from tribal cuisine: an ethno-medicinal, taxonomic, antioxidant and immune-potentiating approach, Food Funct 12 (2021) 4679–4695, https://doi.org/10.1039/D1FO00533B.
[16] S. Khatua, S. Chandra, K. Acharya, Hot alkali extracted antioxidative crude polysaccharide from a novel mushroom enhances immune response via TLR mediated NF-κB activation: a strategy for full utilization of a neglected tribal food, J. Food Biochem. 45 (2021), e13594, https://doi.org/10.1111/jfbc.13594.
[17] S. Ghosh, S. Khatua, A. Dasgupta, K. Acharya, Crude polysaccharide from the milky mushroom, *Calocybe indica* modulates innate immunity of macrophage cells by triggering the MyD88-dependent TLR4/NF-κB pathway, J. Pharm. Pharmacol. 73 (2021) 70–81, https://doi.org/10.1093/jpp/rgaa020.
[18] S. Khatua, K. Acharya, Alkali treated antioxidative crude polysaccharide from *Russula alatoreticula* potentiates murine macrophages by tunning TLR/NF-κB pathway, Sci. Rep. 9 (2019) 1713, https://doi.org/10.1038/s41598-018-37998-2.
[19] S. Khatua, K. Acharya, Water soluble antioxidative crude polysaccharide from *Russula senecis* elicits TLR modulated NF-κB signalling pathway and pro-inflammatory response in murine macrophages, Front. Pharmacol. 9 (2018) 985, https://doi.org/10.3389/fphar.2018.00985.
[20] S. Khatua, K. Dutta, S. Chandra, S. Paloi, K. Das, K. Acharya, Introducing a novel mushroom from mycophagy community with emphasis on biomedical potency, PLoS One 12 (2017), e0178050, https://doi.org/10.1371/journal.pone.0178050.
[21] S. Khatua, K. Acharya, Isolation of crude polysaccharides from *Russula senecis* (Agaricomycetes): characterization, antioxidant activity and immune-enhancing property, Int. J. Med. Mushrooms 23 (2021) 47–57, https://doi.org/10.1615/IntJMedMushrooms.2020037158.
[22] P.O. Magalhães, A.M. Lopes, P.G. Mazzola, C. Rangel-Yagui, T.C.V. Penna, A. Pessoa Jr., Methods of endotoxin removal from biological preparations: a review, J. Pharm. Pharmaceut. Sci. 10 (2007) 388–404.
[23] Q. Yu, S.P. Nie, J.Q. Wang, P.F. Yin, W.J. Li, M.Y. Xie, Polysaccharide from *Ganoderma atrum* induces tumor necrosis factor-α secretion via phosphoinositide 3-kinase/Akt, mitogen-activated protein kinase and nuclear factor-κB signaling pathways in RAW264.7 cells, Int. Immunopharm. 14 (2012) 362–368, https://doi.org/10.1016/j.intimp.2012.09.005.
[24] J. Hirst, G. Jones, M. Cohn, Characterization of a BALB/c myeloma library, J. Immunol. 107 (1971) 926–927.
[25] E.W. Baxter, A.E. Graham, N.A. Re, I.M. Carr, J.I. Robinson, S.L. Mackie, A. W. Morgan, Standardized protocols for differentiation of THP-1 cells to macrophages with distinct M(IFNγ+LPS), M(IL-4) and M(IL-10) phenotypes, J. Immunol. Methods 478 (2020), 112721, https://doi.org/10.1016/j.jim.2019.112721.
[26] D. Wang, Y. Sennari, M. Shen, K. Morita, T. Kanazawa, Y. Yoshida, ERK is involved in the differentiation and function of dimethyl sulfoxide-induced HL-60 neutrophil-like cells, which mimic inflammatory neutrophils, Int. Immunopharm. 84 (2020), 106510, https://doi.org/10.1016/j.intimp.2020.106510.
[27] E. Rincón, B.L. Rocha-Gregg, S.R. Collins, A map of gene expression in neutrophil-like cell lines, BMC Genom. 19 (2018) 573, https://doi.org/10.1186/s12864-018-4957-6.
[28] A. Madhvi, H. Mishra, G.R. Leisching, P.Z. Mahlobo, B. Baker, Comparison of human monocyte derived macrophages and THP1-like macrophages as *in vitro* models for *M. tuberculosis* infection, Comp. Immunol. Microbiol. Infect. Dis. 67 (2019), 101355, https://doi.org/10.1016/j.cimid.2019.101355.
[29] G.R.A. Cabral, Z.T. Wang, L.D. Sibley, R.A. DaMatta, Inhibition of nitric oxide production in activated macrophages caused by *Toxoplasma gondii* infection occurs by distinct mechanisms in different mouse macrophage cell lines, Front. Microbiol. 9 (2018) 1936, https://doi.org/10.3389/fmicb.2018.01936.

[30] W. Chanput, J.J. Mes, H.J. Wichers, THP-1 cell line: an *in vitro* cell model for immune modulation approach, Int. Immunopharm. 23 (2014) 37–45, https://doi.org/10.1016/j.intimp.2014.08.002.

[31] W. Chanput, V. Peters, H. Wichers, THP-1 and U937 cells, in: K. Verhoeckx, et al. (Eds.), The Impact of Food Bioactives on Health, Springer, Cham., 2015, pp. 147–159, https://doi.org/10.1007/978-3-319-16104-4_14.

[32] W. Strober, Trypan blue exclusion test of cell viability, Curr. Protoc. Im. 111 (2015), https://doi.org/10.1002/0471142735.ima03bs21. A3.B.1– A3.B.3.

[33] H.H. Kerschbaum, B.A. Tasa, M. Schürz, K. Oberascher, N. Bresgen, Trypan blue-adapting a dye used for labelling dead cells to visualize pinocytosis in viable cells, Cell. Physiol. Biochem. 55 (2021) 171–184, https://doi.org/10.33594/000000380.

[34]] S.Y. Lyu, W.B. Park, Production of cytokine and NO by RAW 264.7 macrophages and PBMC *in vitro* incubation with flavonoids, Arch Pharm. Res. (Seoul) 28 (2005) 573–581, https://doi.org/10.1007/BF02977761.

[35] P. Wang, S.M. Henning, D. Heber, Limitations of MTT and MTS-based assays for measurement of antiproliferative activity of green tea polyphenols, PLoS One 5 (2010), e10202, https://doi.org/10.1371/journal.pone.0010202.

[36] L. Śliwka, K. Wiktorska, P. Suchocki, M. Milczarek, S. Mielczarek, K. Lubelska, T. Cierpiał, P. Łyżwa, P. Kiełbasiński, A. Jaromin, A. Flis, Z. Chilmonczyk, The comparison of MTT and CVS assays for the assessment of anticancer agent interactions, PLoS One 11 (2016), e0155772, https://doi.org/10.1371/journal.pone.0155772.

[37] E. Vega-Avila, M.K. Pugsley, An overview of colorimetric assay methods used to assess survival or proliferation of mammalian cells, Proc. West. Pharmacol. Soc. 54 (2011) 10–14.

[38] M.V. Berridge, P.M. Herst, A.S. Tan, Tetrazolium dyes as tools in cell biology: new insights into their cellular reduction, Biotechnol. Annu. Rev. 11 (2005) 127–152, https://doi.org/10.1016/S1387-2656(05)11004-7.

[39] Q. Xue, J. Sun, M. Zhao, K. Zhang, R. Lai, Immunostimulatory and anti-tumor activity of a water-soluble polysaccharide from *Phellinus baumii* mycelia, World J. Microbiol. Biotechnol. 27 (2011) 1017–1023, https://doi.org/10.1007/s11274-010-0545-x.

[40] R. Maeda, T. Ida, H. Ihara, T. Sakamoto, Immunostimulatory activity of polysaccharides isolated from *Caulerpa lentillifera* on macrophage cells, Biosci. Biotechnol. Biochem. 76 (2012) 501–505, https://doi.org/10.1271/bbb.110813.

[41] M. Pérez-Recalde, M.C. Matulewicz, C.A. Pujol, M.J. Carlucci, *In vitro* and *in vivo* immunomodulatory activity of sulfated polysaccharides from red seaweed Nemalion helminthoides, Int. J. Biol. Macromol. 63 (2014) 38–42, https://doi.org/10.1016/j.ijbiomac.2013.10.024.

[42] P. Ngamwongsatit, P.P. Banada, W. Panbangred, A.K. Bhunia, WST-1-based cell cytotoxicity assay as a substitute for MTT-based assay for rapid detection of toxigenic *Bacillus* species using CHO cell line, J. Microbiol. Methods 73 (2008) 211–215, https://doi.org/10.1016/j.mimet.2008.03.002.

[43] M. Ishiyama, H. Tominaga, M. Shiga, K. Sasamoto, Y. Ohkura, K. Ueno, A combined assay of cell viability and *in vitro* cytotoxicity with a highly water-soluble tetrazolium salt, neutral red and crystal violet, Biol. Pharm. Bull. 19 (1996) 1518–1520, https://doi.org/10.1248/bpb.19.1518.

[44] J. Qi, S.M. Kim, Characterization and immunomodulatory activities of polysaccharides extracted from green alga *Chlorella ellipsoidea*, Int. J. Biol. Macromol. 95 (2017) 106–114, https://doi.org/10.1016/j.ijbiomac.2016.11.039.

[45] S. Uzunoglu, B. Karaca, H. Atmaca, A. Kisim, C. Sezgin, B. Karabulut, R. Uslu, Comparison of XTT and Alamar blue assays in the assessment of the viability of various human cancer cell lines by AT-101 (-/- gossypol), Toxicol. Mech. Methods 20 (2010) 482–486, https://doi.org/10.3109/15376516.2010.508080.

[46] S. Kim, S. Shin, B. Hyun, H. Kong, S. Han, A. Lee, S. Lee, K. Kim, Immunomodulatory effects of *Dioscoreae* Rhizome against inflammation through suppressed production of cytokines via inhibition of the NF-κB Pathway, Immune Netw 12 (2012) 181–188, https://doi.org/10.4110/in.2012.12.5.181.

[47] D. Gunawardena, K. Shanmugam, M. Low, L. Bennett, S. Govindaraghavan, R. Head, L. Ooi, G. Münch, Determination of anti-inflammatory activities of standardised preparations of plant- and mushroom-based foods, Eur. J. Nutr. 53 (2014) 335–343, https://doi.org/10.1007/s00394-013-0531-9.

[48] L. Zhang, S.R. Koyyalamudi, S.C. Jeong, N. Reddy, P.T. Smith, R. Ananthan, T. Longvah, Antioxidant and immunomodulatory activities of polysaccharides from the roots of *Sanguisorba officinalis*, Int. J. Biol. Macromol. 51 (2012) 1057–1062, https://doi.org/10.1016/j.ijbiomac.2012.08.019.

[49] I.A. Schepetkin, G. Xie, L.N. Kirpotina, R.A. Klein, M.A. Jutila, M.T. Quinn, Macrophage immunomodulatory activity of polysaccharides isolated from *Opuntia polyacantha*, Int. Immunopharm. 8 (2008) 1455–1466, https://doi.org/10.1016/j.intimp.2008.06.003.

[50] V.C. Castro-Alves, D. Gomes, N. Menolli Jr., M.L. Sforça, J.R.O. Nascimento, Characterization and immunomodulatory effects of glucans from *Pleurotus albidus*, a promising species of mushroom for farming and biomass production, Int. J. Biol. Macromol. 95 (2017) 215–223, https://doi.org/10.1016/j.ijbiomac.2016.11.059.

[51] H.Y. Cui, C.L. Wang, Y.R. Wang, Z.J. Li, Y.N. Zhang, The polysaccharide isolated from *Pleurotus nebrodensis* (PN-S) shows immune-stimulating activity in RAW264.7 macrophages, Chin. J. Nat. Med. 13 (2015) 355–360, https://doi.org/10.1016/S1875-5364(15)30026-1.

[52] M.C. Pereira, E.F. Nodari, M.R. de Abreu, L.N. Paiatto, P.U. Simioni, M. I. Camargo-Mathias, *Rhipicephalus sanguineus* salivary gland extract as a source of immunomodulatory molecules, Exp. Appl. Acarol. 83 (2021) 387–398, https://doi.org/10.1007/s10493-021-00591-w.

[53] S. Ghosh, S. Khatua, K. Acharya, Crude polysaccharide from wild mushroom enhances immune response in murine macrophage cells by TLR/NF-κB pathway, J. Pharm. Pharmacol. 71 (2019) 1311–1323, https://doi.org/10.1111/jphp.13104.

[54] R.S. Wu, K.C. Liu, N.Y. Tang, H.K. Chung, S.W. Ip, J.S. Yang, J.G. Chung, cDNA microarray analysis of the gene expression of murine leukemia RAW 264.7 cells after exposure to propofol, Environ. Toxicol. 28 (2013) 471–478, https://doi.org/10.1002/tox.20742.

[55] S. Bancos, D.L. Stevens, K.M. Tyner, Effect of silica and gold nanoparticles on macrophage proliferation, activation markers, cytokine production, and phagocytosis *in vitro*, Int. J. Nanomed. 10 (2015) 183–206, https://doi.org/10.2147/IJN.S72580.

[56] S. Jiang, H. Yin, X. Qi, W. Song, W. Shi, J. Mou, J. Yang, Immunomodulatory effects of fucosylated chondroitin sulfate from *Stichopus chloronotus* on RAW 264.7 cells, Carbohydr. Polym. 251 (2021), 117088, https://doi.org/10.1016/j.carbpol.2020.117088.

[57] C.A. Janeway Jr., P. Travers, M. Walport, M. Shlomchik, Immunobiology: the Immune System in Health and Disease, Garland Science Publishing, New York, 2005.

[58] T.S. Kapellos, L. Taylor, H. Lee, S.A. Cowley, W.S. James, A.J. Iqbal, D.R. Greaves, A novel real time imaging platform to quantify macrophage phagocytosis, Biochem. Pharmacol. 116 (2016) 107–119, https://doi.org/10.1016/j.bcp.2016.07.011.

[59] V. Geetha, S. Arumugam, M. Doble, Synthesis, characterization, and biological activity of aminated zymosan, ACS Omega 5 (2020) 15973–15982, https://doi.org/10.1021/acsomega.0c01243.

[60] L.B. Sigola, A.L. Fuentes, L.M. Millis, J. Vapenik, A. Murira, Effects of Toll-like receptor ligands on RAW 264.7 macrophage morphology and zymosan phagocytosis, Tissue Cell 48 (2016) 389–396, https://doi.org/10.1016/j.tice.2016.04.002.

[61] P. More, K. Pai, Effect of *Tinospora cordifoia* (Guduchi) on the phagocytic and pinocytic activity of murine macrophages *in vitro*, Indian J. Exp. Biol. 55 (2017) 21–26.

[62] F.N. Razali, A. Ismail, N.Z. Abidin, A.S. Shuib, Stimulatory effects of polysaccharide fraction from *Solanum nigrum* on RAW 264.7 murine macrophage cells, PLoS One 9 (2014), e108988, https://doi.org/10.1371/journal.pone.0108988.

[63] S. Jiang, H. Yin, X. Qi, W. Song, W. Shi, J. Mou, J. Yang, Immunomodulatory effects of fucosylated chondroitin sulfate from *Stichopus chloronotus* on RAW 264.7 cells, Carbohydr. Polym. 251 (2021), 117088, https://doi.org/10.1016/j.carbpol.2020.117088.

[64] P. Nunes, N. Demaurex, The role of calcium signaling in phagocytosis, J. Leukoc. Biol. 88 (2010) 57–68, https://doi.org/10.1189/jlb.0110028.

[65] J.Y. Lee, Y.J. Kim, H.J. Kim, Y.S. Kim, W. Park, Immunostimulatory effect of Laminarin on RAW 264.7 mouse macrophages, Molecules 17 (2012) 5404–5411, https://doi.org/10.3390/molecules17055404.

[66] F. Di Virgilio, L.H. Jiang, S. Roger, S. Falzoni, A.C. Sarti, V. Vultaggio-Poma, P. Chiozzi, E. Adinolfi, Structure, function and techniques of investigation of the P2X7 receptor (P2X7R) in mammalian cells, Methods Enzymol. 629 (2019) 115–150, https://doi.org/10.1016/bs.mie.2019.07.043.

[67] M. Lévêque, A. Penna, S. Le Trionnaire, C. Belleguic, B. Desrues, G. Brinchault, S. Jouneau, D. Lagadic-Gossmann, C. Martin-Chouly, Phagocytosis depends on TRPV2-mediated calcium influx and requires TRPV2 in lipids rafts: alteration in macrophages from patients with cystic fibrosis, Sci. Rep. 8 (2018) 4310, https://doi.org/10.1038/s41598-018-22558-5.

[68] M. Harada, T. Kuda, S. Nakamura, G. Lee, H. Takahashi, B. Kimura, *In vitro* antioxidant and immunomodulation capacities of low-molecular weight-alginate-and laminaran-responsible gut indigenous bacteria, LWT - Food Sci. Technol. (Lebensmittel-Wissenschaft -Technol.) 151 (2021), 112127, https://doi.org/10.1016/j.lwt.2021.112127.

[69] J. Sun, X. Zhang, M. Broderick, H. Fein, Measurement of nitric oxide production in biological systems by using Griess reaction assay, Sensors 3 (2003) 276–284, https://doi.org/10.3390/s30800276.

[70] R.T. Makola, J. Kgaladi, G.K. More, P. Jansen van Vuren, J.T. Paweska, T. M. Matsebatlela, Lithium inhibits NF-κB nuclear translocation and modulate inflammation profiles in Rift valley fever virus-infected Raw 264.7 macrophages, Virol. J. 18 (2021) 116, https://doi.org/10.1186/s12985-021-01579-z.

[71] M. Herb, A. Gluschko, M. Schramm, Reactive oxygen species: not omnipresent but important in many locations, Front. Cell Dev. Biol. 9 (2021), 716406, https://doi.org/10.3389/fcell.2021.716406.

[72] P.M. Mortimer, S.A. Mc Intyre, D.C. Thomas, Beyond the extra respiration of phagocytosis: NADPH oxidase 2 in adaptive immunity and inflammation, Front. Immunol. 12 (2021), 733918, https://doi.org/10.3389/fimmu.2021.733918.

[73] E. Rendra, V. Riabov, D.M. Mossel, T. Sevastyanova, M.C. Harmsen, J. Kzhyshkowska, Reactive oxygen species (ROS) in macrophage activation and function in diabetes, Immunobiology 224 (2019) 242–253, https://doi.org/10.1016/j.imbio.2018.11.010.

[74] L. Liu, H. Li, R. Xu, P. Li, Expolysaccharides from *Bifidobacterium animalis* RH activates RAW 264.7 macrophages through toll-like receptor 4, Food Agric. Immunol. 28 (2017) 149–161, https://doi.org/10.1080/09540105.2016.1230599.

[75] J.J. Yang, Y.H. Wang, J. Yin, H. Leng, S.D. Shen, Polysaccharides from *Ulva prolifera* O.F. Müller inhibit cell proliferation via activating MAPK signaling in A549 and H1650 cells, Food Funct 12 (2021) 6915–6924, https://doi.org/10.1039/d1fo00294e.

[76] S. Shoaib, S. Tufail, M.A. Sherwani, N. Yusuf, N. Islam, Phenethyl isothiocyanate induces apoptosis through ROS generation and Caspase-3 activation in cervical

cancer cells, Front. Pharmacol. 12 (2021), 673103, https://doi.org/10.3389/fphar.2021.673103.
[77] J. Deng, Z. Li, Z. Mo, S. Xu, H. Mao, D. Shi, Z. Li, X. Dan, X. Luo, Immunomodulatory effects of N-Acetyl chitooligosaccharides on RAW264.7 macrophages, Mar. Drugs 18 (2020) 421, https://doi.org/10.3390/md18080421.
[78] D.D. Smolyarova, O.V. Podgorny, D.S. Bilan, V.V. Belousov, A guide to genetically encoded tools for the study of H_2O_2, FEBS J. (2021), https://doi.org/10.1111/febs.16088.
[79] N. Nakao, T. Kurokawa, T. Nonami, G. Tumurkhuu, N. Koide, T. Yokochi, Hydrogen peroxide induces the production of tumor necrosis factor-alpha in RAW 264.7 macrophage cells via activation of p38 and stress-activated protein kinase, Innate Immun. 14 (2008) 190–196, https://doi.org/10.1177/1753425908093932.
[80] S.C. Sargi, M.M. Dalalio, J.V. Visentainer, R.C. Bezerra, J.Â. Perini, F. B. Stevanato, J.E. Visentainer, Production of TNF-α, nitric oxide and hydrogen peroxide by macrophages from mice with paracoccidioidomycosis that were fed a linseed oil-enriched diet, Mem. Inst. Oswaldo Cruz 107 (2012) 303–309, https://doi.org/10.1590/s0074-02762012000300003.
[81] Y. Mokhtari, A. Pourbagheri-Sigaroodi, P. Zafari, N. Bagheri, S.H. Ghaffari, D. Bashash, Toll-like receptors (TLRs): an old family of immune receptors with a new face in cancer pathogenesis, J. Cell Mol. Med. 25 (2021) 639–651, https://doi.org/10.1111/jcmm.16214.
[82] T. Kawasaki, T. Kawai, Toll-like receptor signaling pathways, Front. Immunol. 5 (2014) 461, https://doi.org/10.3389/fimmu.2014.00461.
[83] S.A. Richard, Exploring the pivotal immunomodulatory and anti-inflammatory potentials of glycyrrhizic and glycyrrhetinic acids, Mediat. Inflamm. 2021 (2021), 6699560, https://doi.org/10.1155/2021/6699560.
[84] A. Gruden-Movsesijan, LjS. Milosavljevic, The involvement of the macrophage mannose receptor in the innate immune response to infection with parasite *Trichinella spiralis*, Vet. Immunol. Immunopathol. 109 (2006) 57–67, https://doi.org/10.1016/j.vetimm.2005.07.022.
[85] C.F. Ellefsen, C.W. Wold, A.L. Wilkins, F. Rise, A.B.C. Samuelsen, Water-soluble polysaccharides from *Pleurotus eryngii* fruiting bodies, their activity and affinity for Toll-like receptor 2 and dectin-1, Carbohydr. Polym. 264 (2021), 117991, https://doi.org/10.1016/j.carbpol.2021.117991.
[86] S.K. Seong, H.W. Kim, Potentiation of innate immunity by β-glucans, MYCOBIOLOGY 38 (2010) 144–148, https://doi.org/10.4489/MYCO.2010.38.2.144.
[87] J.W. Kim, J. Lee, A.Y. Yoo, J.W. Choi, Y.I. Park, J.K. Park, Immune-stimulating activity of water-soluble extracellular polysaccharide isolated from *Rhizobium massiliae*, Process Biochem. 63 (2017) 236–243, https://doi.org/10.1016/j.procbio.2017.09.005.
[88] V. Premkumar, M. Dey, R. Dorn, I. Raskin, MyD88-dependent and independent pathways of Toll-Like Receptors are engaged in biological activity of Triptolide in ligand-stimulated macrophages, BMC Chem. Biol. 10 (2010) 3, https://doi.org/10.1186/1472-6769-10-3.
[89] N.G. Geum, H.J. Eo, H.J. Kim, G.H. Park, H.J. Son, J.B. Jeong, Immune-enhancing activity of Hydrangea macrophylla subsp. serrata leaves through TLR4/ROS-dependent activation of JNK and NF-κB in RAW264.7 cells and immunosuppressed mice, J. Funct. Foods 73 (2020), 104139, https://doi.org/10.1016/j.jff.2020.104139.
[90] C. Monmai, W. Rod-in, A. Jang, S. Lee, S.K. Jung, S. You, W.J. Park, Immune-enhancing effects of anionic macromolecules extracted from *Codium fragile* coupled with arachidonic acid in RAW264.7 cells, PLoS One 15 (2020), e0239422, https://doi.org/10.1371/journal.pone.0239422.
[91] H. Sun, X. Ni, D. Zeng, F. Zou, M. Yang, Z. Peng, Y. Zhou, Y. Zeng, H. Zhu, H. Wang, Z. Yin, K. Pan, B. Jing, Bidirectional immunomodulating activity of fermented polysaccharides from Yupingfeng, Res. Vet. Sci. 110 (2017) 22–28, https://doi.org/10.1016/j.rvsc.2016.10.015.
[92] S.L. Fu, Y.H. Hsu, P.Y. Lee, W.C. Hou, L.C. Hung, C.H. Lin, C.M. Chen, Y.J. Huang, Dioscorin isolated from *Dioscorea alata* activates TLR4-signaling pathways and induces cytokine expression in macrophages, Biochem. Biophys. Res. Commun. 339 (2006) 137–144, https://doi.org/10.1016/j.bbrc.2005.11.005.
[93] Y. Pan, X. Zhao, S.H. Kim, S.A. Kang, Y.G. Kim, K.Y. Park, Anti-inflammatory effects of Beopje curly dock (*Rumex crispus* L.) in LPS-induced RAW 264.7 cells and its active compounds, J. Food Biochem. 44 (2020), e13291, https://doi.org/10.1111/jfbc.13291.
[94] G. Yi, H. Li, M. Liu, Z. Ying, J. Zhang, X. Liu, Soybean protein-derived peptides inhibit inflammation in LPS-induced RAW264.7 macrophages via the suppression of TLR4-mediated MAPK-JNK and NF-kappa B activation, J. Food Biochem. 44 (2020), e13289, https://doi.org/10.1111/jfbc.13289.
[95] S. Feng, H. Ding, L. Liu, C. Peng, Y. Huang, F. Zhong, W. Li, T. Meng, J. Li, X. Wang, Y. Li, J. Wu, *Astragalus* polysaccharide enhances the immune function of RAW264.7 macrophages via the NF-κB p65/MAPK signaling pathway, Exp. Ther. Med. 21 (2021) 1–20, https://doi.org/10.3892/etm.2020.9452.
[96] M. Tabarsa, E.H. Dabaghian, S. You, K. Yelithao, S. Palanisamy, N.M. Prabhu, C. Li, Inducing inflammatory response in RAW264.7 and NK-92 cells by an arabinogalactan isolated from *Ferula gummosa* via NF-κB and MAPK signaling pathways, Carbohydr. Polym. 241 (2020), 116358, https://doi.org/10.1016/j.carbpol.2020.116358.
[97] C.K. Youn, S.J. Park, M.Y. Lee, M.J. Cha, O.H. Kim, H.J. You, I.Y. Chang, S. P. Yoon, Y.J. Jeon, Silibinin inhibits LPS-induced macrophage activation by blocking p38 MAPK in RAW 264.7 cells, Biomol. Ther. 21 (2013) 258–263, https://doi.org/10.4062/biomolther.2013.044.
[98] J.Y. Lee, J.Y. Kim, Y.G. Lee, M.H. Rhee, E.K. Hong, J.Y. Cho, Molecular mechanism of macrophage activation by exopolysaccharides from liquid culture of *Lentinus edodes*, J. Microbiol. Biotechnol. 18 (2008) 355–364.
[99] M. Wang, X. Yang, J. Zhao, C. Lu, W. Zhu, Structural characterization and macrophage immunomodulatory activity of a novel polysaccharide from *Smilax glabra* Roxb, Carbohydr. Polym. 156 (2017) 390–402, https://doi.org/10.1016/j.carbpol.2016.09.033.
[100] T.A. Trinh, J. Park, J.H. Oh, J.S. Park, D. Lee, C.E. Kim, H.S. Choi, S.B. Kim, G. S. Hwang, B.A. Koo, K.S. Kang, Effect of herbal formulation on immune response enhancement in RAW 264.7 macrophages, Biomolecules 10 (2020) 424, https://doi.org/10.3390/biom10030424.
[101] J.S. Lee, A. Synytsya, H.B. Kim, D.J. Choi, S. Lee, J. Lee, W.J. Kim, S. Jang, Y. I. Park, Purification, characterization and immunomodulating activity of a pectic polysaccharide isolated from Korean mulberry fruit Oddi (*Morus alba* L.), Int. Immunopharm. 17 (2013) 858–866, https://doi.org/10.1016/j.intimp.2013.09.019.
[102] H.E. Park, K.H. Do, W.K. Lee, The immune-modulating effects of viable *Weissella cibaria* JW15 on RAW 264.7 macrophage cells, J. Biomed. Res. 34 (2020) 36–43, https://doi.org/10.7555/JBR.33.20190095.
[103] Y. Sugiyama, Y. Hiraiwa, Y. Hagiya, M. Nakajima, T. Tanaka, S. Ogura, 5-Aminolevulinic acid regulates the immune response in LPS-stimulated RAW 264.7 macrophages, BMC Immunol. 19 (2018) 41, https://doi.org/10.1186/s12865-018-0277-5.
[104] Y. Hou, X. Ding, W. Hou, B. Song, T. Wang, F. Wang, J. Zhong, Immunostimulant activity of a novel polysaccharide isolated from *Lactarius deliciosus* (L. ex Fr.) Gray, Indian, J. Pharmacol. Sci. 75 (2013) 393–399, https://doi.org/10.4103/0250-474X.119809.
[105] J. Kim, Y. Lee, H. Kong, Y. Song, L. Chong-Kil, K. Kyungjae, Immunomodulatory effects of *Aloe saponaria* on lipopolysaccharide-activated RAW 264.7 macrophages, Nat. Prod. Chem. Res. 4 (2016) 6, https://doi.org/10.4172/2329-6836.1000243.
[106] L. Teng, H. Fu, M. Wang, C. Deng, J. Chen, Stimulation of RAW264.7 macrophages by sulfated *Escherichia coli* K5 capsular polysaccharide *in vitro*, Mol. Med. Rep. 12 (2015) 5545–5553, https://doi.org/10.3892/mmr.2015.4082.
[107] X. Xu, X. Wu, Q. Wang, N. Cai, H. Zhang, Z. Jiang, M. Wan, T. Oda, Immunomodulatory effects of alginate oligosaccharides on murine macrophage RAW264.7 cells and their structure-activity relationships, J. Agric. Food Chem. 62 (2014) 3168–3176, https://doi.org/10.1021/jf405633n.
[108] D. Huang, L. Yang, C. Wang, S. Ma, L. Cui, S. Huang, X. Sheng, Q. Weng, M. Xu, Immunostimulatory activity of protein hydrolysate from oviductus ranae on macrophage *in vitro*, Evid. Based Complement. Alternat. Med. 2014 (2014), 180234, https://doi.org/10.1155/2014/180234.
[109] T. Yayeh, W.J. Oh, S.C. Park, T.H. Kim, J.Y. Cho, H.J. Park, I.K. Lee, S.K. Kim, S. B. Hong, B.S. Yun, M.H. Rhee, *Phellinus baumii* ethyl acetate extract inhibits lipopolysaccharide-induced iNOS, COX-2, and proinflammatory cytokine expression in RAW264.7 cells, J. Nat. Med. 66 (2012) 49–54, https://doi.org/10.1007/s11418-011-0552-8.
[110] G. Gong, F. Xie, Y. Zheng, W. Hu, B. Qi, H. He, T.T. Dong, K.W. Tsim, The effect of methanol extract from *Saussurea involucrata* in the lipopolysaccharide-stimulated inflammation in cultured RAW 264.7 cells, J. Ethnopharmacol. 251 (2020) 112532, https://doi.org/10.1016/j.jep.2019.112532.
[111] J.M. Kang, W.G. Yoo, H.G. Lê, J. Lee, W. Sohn, B. Na, *Clonorchis sinensis* MF6p/HDM (CsMF6p/HDM) induces pro-inflammatory immune response in RAW 264.7 macrophage cells via NF-κB-dependent MAPK pathways, Parasites Vectors 13 (2020) 20, https://doi.org/10.1186/s13071-020-3882-0.
[112] R.A. Sueiro-Benavides, J.M. Leiro-Vidal, A.Á. Salas-Sánchez, J.A. Rodríguez-González, F.J. Ares-Pena, M.E. López-Martín, Radiofrequency at 2.45 GHz increases toxicity, pro-inflammatory and pre-apoptotic activity caused by black carbon in the RAW 264.7 macrophage cell line, Sci. Total Environ. 765 (2020), 142681, https://doi.org/10.1016/j.scitotenv.2020.142681.
[113] L. Chen, P. Chen, J. Liu, C. Hu, S. Yang, D. He, P. Yu, M. Wu, X. Zhang, *Sargassum fusiforme* polysaccharide SFP–F2 activates the NF-κB signaling pathway via CD14/IKK and P38 axes in RAW264.7 cells, Mar. Drugs 16 (2018) 264, https://doi.org/10.3390/md16080264.
[114] T. Shen, G. Wang, L. You, L. Zhang, H. Ren, W. Hu, Q. Qiang, X. Wang, L. Ji, Z. Gu, X. Zhao, Polysaccharide from wheat bran induces cytokine expression via the Toll-like receptor 4-mediated p38 MAPK signaling pathway and prevents cyclophosphamide-induced immunosuppression in mice, Food Nutr. Res. 61 (2017), 1344523, https://doi.org/10.1080/16546628.2017.1344523.
[115] Z. Ji, Q. Tang, J. Zhang, Y. Yang, W. Jia, Y. Pan, Immunomodulation of RAW264.7 macrophages by GLIS, a proteopolysaccharide from *Ganoderma lucidum*, J. Ethnopharmacol. 112 (2007) 445–450, https://doi.org/10.1016/j.jep.2007.03.035.
[116] S.H. Vu, A.W. Bernardo Reyes, T.X. Ngoc Huy, W. Min, H.J. Lee, H.J. Kim, J. H. Lee, S. Kim, Prostaglandin I2 (PGI2) inhibits Brucella abortus internalization in macrophages via PGI2 receptor signaling, and its analogue affects immune response and disease outcome in mice, Dev. Comp. Immunol. 115 (2021), 103902, https://doi.org/10.1016/j.dci.2020.103902.
[117] H.H. Lee, J.S. Lee, J.Y. Cho, Y.E. Kim, E.K. Hong, Structural characteristics of immunostimulating polysaccharides from *Lentinus edodes*, J. Microbiol. Biotechnol. 19 (2009) 455–461, https://doi.org/10.4014/jmb.0809.542.
[118] S. Suraiya, W.J. Jang, H.J. Cho, Y.B. Choi, H.D. Park, J.-M. Kim, I.-S. Kong, Immunomodulatory effects of *Monascus* spp.-fermented *Saccharina japonica* extracts on the cytokine gene expression of THP-1 cells, Appl. Biochem. Biotechnol. 188 (2019) 498–513, https://doi.org/10.1007/s12010-018-02930-x.

[119] P. Li, H. Wang, Q. Shao, B. Kong, X. Qu, Fucoidan modulates cytokine production and migration of THP-1-derived macrophages via colony-stimulating factor-1, Mol. Med. Rep. 15 (2017) 2325–2332, https://doi.org/10.3892/mmr.2017.6228.
[120] M. Hasani, N.A. Sani, B. Khodabakhshi, M.S. Arabi, S. Mohammadi, Y. Yazdani, Encapsulation of Leflunomide (LFD) in a novel niosomal formulation facilitated its delivery to THP-1 monocytic cells and enhanced Aryl hydrocarbon receptor (AhR) nuclear translocation and activation, Daru 27 (2019) 635–644, https://doi.org/10.1007/s40199-019-00293-0.
[121] T.X. Hoang, J.H. Jung, J.Y. Kim, All-trans retinoic acid enhances bacterial flagellin-stimulated proinflammatory responses in human monocyte THP-1 cells by upregulating CD14, Biomed, Res. Int. 2019 (2019), 8059312, https://doi.org/10.1155/2019/8059312.
[122] L. Sun, X. Li, M. Xu, F. Yang, W. Wang, X. Niu, *In vitro* immunomodulation of magnesium on monocytic cell toward anti-inflammatory macrophages, Regen. Biomater. 7 (2020) 391–401, https://doi.org/10.1093/rb/rbaa010.
[123] H.Y. Qi, J.H. Shelhamer, Toll-like receptor 4 signaling regulates cytosolic phospholipase A2 activation and lipid generation in lipopolysaccharide-stimulated macrophages, J. Biol. Chem. 280 (2005) 38969–38975, https://doi.org/10.1074/jbc.M509352200.
[124] H. Wang, J. Zhang, H. Wu, C. Jiang, Q. Zheng, Z. Li, Inhibition of RAW264.7 macrophage inflammatory cytokines release by small hairpin RNAi targeting TLR4, J. Huazhong Univ. Sci. Technolog. Med. Sci. 26 (5) (2006) 500–503, https://doi.org/10.1007/s11596-006-0503-x.
[125] O. Ernst, S.J. Vayttaden, I.D.C. Fraser, Measurement of NF-κB activation in TLR-activated macrophages, Methods Mol. Biol. 1714 (2018) 67–78, https://doi.org/10.1007/978-1-4939-7519-8_5.
[126] S. Matsuo, S. Yamazaki, K. Takeshige, T. Muta, Crucial roles of binding sites for NF-κB and C/EBPs in IκB-ζ-mediated transcriptional activation, Biochem. J. 405 (2007) 605–615, https://doi.org/10.1042/BJ20061797.
[127] C. Guo, J. Bi, X. Li, J. Lyu, X. Liu, X. Wu, J. Liu, Immunomodulation effects of polyphenols from thinned peach treated by different drying methods on RAW264.7 cells through the NF-κB and Nrf2 pathways, Food Chem. 340 (2021), 127931, https://doi.org/10.1016/j.foodchem.2020.127931.
[128] L. Zha, J. Chen, S. Sun, L. Mao, X. Chu, H. Deng, J. Cai, X. Li, Z. Liu, W. Cao, Soyasaponins can blunt inflammation by inhibiting the reactive oxygen species-mediated activation of PI3K/Akt/NF-kB pathway, PLoS One 9 (2014), e107655, https://doi.org/10.1371/journal.pone.0107655.
[129] J. Lee, M.H. Rhee, E. Kim, J.Y. Cho, BAY 11-7082 is a broad-spectrum inhibitor with anti-inflammatory activity against multiple targets, Mediat. Inflamm. (2012), 416036, https://doi.org/10.1155/2012/416036, 2012.
[130] N.S. Holden, C.E. Tacon, Principles and problems of the electrophoretic mobility shift assay, J. Pharmacol. Toxicol. Methods 63 (2011) 7–14, https://doi.org/10.1016/j.vascn.2010.03.002.
[131] D. Haydar, T.J. Cory, S.E. Birket, B.S. Murphy, K.R. Pennypacker, A.P. Sinai, D. J. Feola, Azithromycin polarizes macrophages to an M2 phenotype via inhibition of the STAT1 and NF-κB signaling pathways, J. Immunol. 203 (2019) 1021–1030, https://doi.org/10.4049/jimmunol.1801228.
[132] K.B. Megha, X. Joseph, V. Akhil, P.V. Mohanan, Cascade of immune mechanism and consequences of inflammatory disorders, Phytomedicine 91 (2021), 153712, https://doi.org/10.1016/j.phymed.2021.153712.
[133] A. Hariharan, A.R. Hakeem, S. Radhakrishnan, M.S. Reddy, M. Rela, The role and therapeutic potential of NF-kappa-B pathway in severe COVID-19 patients, Inflammopharmacology 29 (2021) 91–100, https://doi.org/10.1007/s10787-020-00773-9.
[134] S. Ramaswami, M.S. Hayden, Electrophoretic mobility shift assay analysis of NF-κB DNA binding, in: M. May (Ed.), NF-kappa B. Methods in Molecular Biology, Humana Press, New York, NY, 2015, https://doi.org/10.1007/978-1-4939-2422-6_1.
[135] S.-H. Baek, T. Park, M.-G. Kang, D. Park, Anti-inflammatory activity and ROS regulation effect of Sinapaldehyde in LPS-stimulated RAW 264.7 macrophages, Molecules 25 (2020) 4089, https://doi.org/10.3390/molecules25184089.
[136] S. Bahramzadeh, M. Tabarsa, S. You, K. Yelithao, V. Klochkov, R. Ilfat, An arabinogalactan isolated from *Boswellia carterii*: purification, structural elucidation and macrophage stimulation via NF-κB and MAPK pathways, J. Funct. Foods. 52 (2019) 450–458, https://doi.org/10.1016/j.jff.2018.11.025.
[137] Y. Liu, X. Wu, W. Jin, Y. Guo, Immunomodulatory effects of a low-molecular weight polysaccharide from *Enteromorpha prolifera* on Raw 264.7 macrophages and cyclophosphamide-induced immunosuppression mouse models, Mar. Drugs 18 (2020) 340, https://doi.org/10.3390/md18070340.
[138] N.F.Z. Zailan, N. Jaganathan, T. Sandramuti, S.N.E. Sarchio, M. Hassan, Inhibition of GSK-3 by Tideglusib suppresses activated macrophages and inflammatory responses in lipopolysaccharide-stimulated RAW 264.7 cell line, Malaysian J. Med. Health Sci. 16 (2020) 2–8.
[139] E. Khodadadi, L. Fahmideh, E. Khodadadi, S. Dao, M. Yousefi, S. Taghizadeh, M. Asgharzadeh, B. Yousefi, H.S. Kafil, Current advances in DNA methylation analysis methods, BioMed Res. Int. 2021 (2021), 8827516, https://doi.org/10.1155/2021/8827516.